University of Groningen

Structure and Dynamics of the Lowest Triplet State in p-Benzoquinone I. An isotope effect study on the optical absorption, emission and ODMR spectra

Veenvliet, Hendrik; Wiersma, Douwe A.

Published in:
Chemical Physics

DOI:
10.1016/0301-0104(75)80155-8

IMPORTANT NOTE: You are advised to consult the publisher's version (publisher's PDF) if you wish to cite from it. Please check the document version below.

Document Version
Publisher's PDF, also known as Version of record

Publication date:
1975

Link to publication in University of Groningen/UMCG research database

Citation for published version (APA):
Veenvliet, H., & Wiersma, D. A. (1975). Structure and Dynamics of the Lowest Triplet State in p-Benzoquinone I. An isotope effect study on the optical absorption, emission and ODMR spectra. Chemical Physics, 8(3). DOI: 10.1016/0301-0104(75)80155-8

Copyright
Other than for strictly personal use, it is not permitted to download or to forward/distribute the text or part of it without the consent of the author(s) and/or copyright holder(s), unless the work is under an open content license (like Creative Commons).

Take-down policy
If you believe that this document breaches copyright please contact us providing details, and we will remove access to the work immediately and investigate your claim.

Downloaded from the University of Groningen/UMCG research database (Pure): http://www.rug.nl/research/portal. For technical reasons the number of authors shown on this cover page is limited to 10 maximum.

Download date: 11-02-2018

Chemical Physics 8 (1975) 432–457
© North-Holland Publishing Company

STRUCTURE AND DYNAMICS OF THE LOWEST TRIPLET STATE IN p-BENZOQUINONE

I. An isotope effect study on the optical absorption, emission and ODMR spectra

Hendrik VEENVLIET and Douwe A. WIERSMA
Laboratory for Physical Chemistry, University of Groningen, Zernikelaan, Paddepoel, Groningen, The Netherlands

Received 15 November 1974

The results of detailed spectroscopic experiments on the lowest $n\pi^*$ triplet state of *p*-benzoquinone-h_4, -dh_3, 2,6-d_2h_2, -d_4, and -CH_3 in mixed and isotopic mixed crystals are presented and analyzed. The origin of the lowest B_{1g} ($n\pi^*$) singlet–triplet transition in *p*-benzoquinone-h_4 (PBQ-h_4) is shown to be induced by asymmetric isotopic substitution and the oscillator strength of this origin is seen to be accounted for by a corresponding decrease in intensity of a level 16.9 cm^{-1} higher in energy in the pure PBQ-h_4 crystal. The combined oscillator strength of these close lying levels is measured and found to be almost independent of deuteration.

These results are discussed in reference to the previously proposed double minimum potential model for the lowest $n\pi^*$ triplet state in PBQ-h_4 and the applicability of this model is critically examined.

Optical absorption experiments on heavily doped isotopic mixed crystals of PBQ-h_4 in PBQ-d_4 show hydrogen (deuterium) bonding effects between translational inequivalent molecules to be primarily responsible for the observed cluster states. These hydrogen bonding effects also induce the electronic origin of the B_{1g} ($n\pi^*$) triplet state in case of a translational inequivalent dimer.

A detailed vibrational analysis of the phosphorescence spectrum of PBQ-h_4 in a PBQ-d_4 host crystal at 1.8 K is presented and it is shown that the unobserved origin of the B_{1g} ($n\pi^*$) triplet state of PBQ-h_4 is located at 18609 ± 1 cm^{-1} and that the inversion splitting in this lowest excited state amounts to 21 ± 1 cm^{-1} in this mixed crystal system. An isotope effect study on the vibronic structure in the emission spectrum further indicates that the excited state structure of PBQ is isotope dependent.

The observed large isotope effect on the ZFS parameters of the lowest triplet state of PBQ-h_4 is demonstrated to be an intramolecular phenomenon and explained as an isotope dependent spin–orbit contribution to the ZFS parameters, induced by localization of the $n\pi^*$ excitation on oxygen.

Finally the dynamics of energy migration in the dilute PBQ-h_4 in PBQ-d_4 isotopic mixed crystal is probed by concentration and temperature dependent phosphorescence intensity measurements and it is suggested that trap–exciton band communication effects are of importance in this system.

1. Introduction

One of the more persisting spectroscopic problems in the past decade has been the assignment and analysis of the visible absorptions of *p*-benzoquinone (PBQ; $L = z(b_{1u})$, $M = y(b_{2u})$). Sidman[1], in a paper reporting the first low temperature spectroscopic measurements on PBQ-h_4 crystals, already proposed that the visible absorptions of PBQ-h_4 were caused by promotions of oxygen lone pair electrons into the quinoid system. PBQ-h_4 contains two such oxygen lone pairs, related by inversion, and therefore singlet and triplet $n\pi^*$ excitations of g and u symmetry can be formed. Furthermore the PBQ-h_4 crystal structure is such [2] that the molecule retains its center of inversion and therefore the parity of the electronically excited states in PBQ-h_4 is strictly conserved in the crystal. The difficulty in the assignment of the lower electronic states of PBQ-h_4, in retrospect, is the occurrence of four singlet and triplet $n\pi^*$ states in a narrow energy span of 2000 cm^{-1}.

Trommsdorff [3] recently summarized all experimental evidence that supports an ordering of the lower excited states in PBQ-h_4 as shown in fig. 1. The B_{1g} and

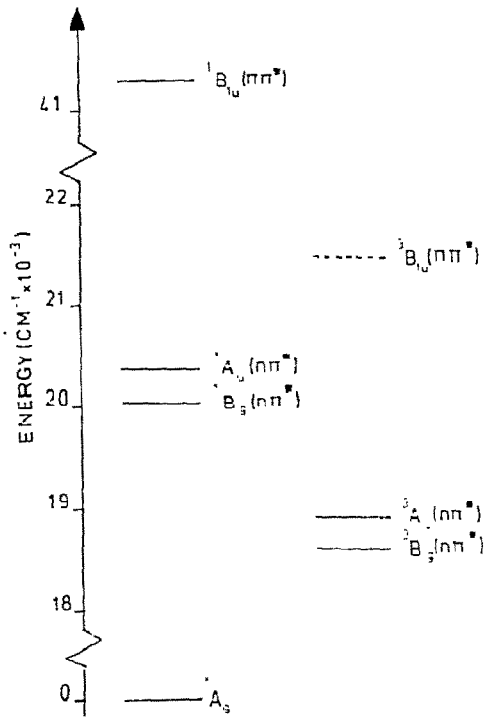

Fig. 1. Jablonski diagram for crystalline PBQ-h_4. The data in this figure have been taken from ref. [3].

A_u $n\pi^*$ triplet states are split by some 340 cm^{-1} and the corresponding singlet states by 255 cm^{-1}. In such a situation strong vibronic coupling effects are expected to occur [4] that may lead to a pseudo Jahn–Teller instability of the lowest excited state, and indeed the observation, by means of the Stark effect [5,6], of close lying levels of opposite parity in both the lowest triplet and singlet state absorption region of PBQ-h_4 crystals led to the proposal that both the lowest triplet and singlet $n\pi^*$ states in PBQ-h_4 had acquired a double minimum potential (DMP) well along b_{1u} type nuclear motions. The close lying levels of opposite parity were assigned as inversion levels of this DMP well. In a recent paper by Dunn and Francis [7] these inversion levels in the lowest $n\pi^*$ singlet state absorption region however were assigned as the electronic origins of the B_{1g} and A_u $n\pi^*$ singlet states. In this paper we will not discuss the controversy in assignment of the absorptions in the lowest singlet state region, but restrict ourselves to a discussion of the spectroscopic properties of the lowest triplet state. In a recent communication [8] we reported the results of ODMR experiments on single vibronic levels in the phosphorescence spectrum of PBQ-h_4 in a PBQ-d_4 mixed crystal thereby confirming the assignment of the lowest triplet state in PBQ-h_4 as the B_{1g} ($n\pi^*$) triplet state.

In this paper we will present and discuss the results of an isotope effect study on the optical absorption, phosphorescence and ODMR spectra of the lowest B_{1g} ($n\pi^*$) triplet state of PBQ-h_4.

In section 2 and 3 of this paper the observed isotope effects on the absorption and phosphorescence spectra are used to critically examine the applicability of the DMP model in explaining the effects observed. In section 2 it is also demonstrated that hydrogen (deuterium) bonding effects play an important role in the absorption and emission spectra of PBQ-h_4 in PBQ-d_4 isotopic mixed crystals.

In section 3 we further discuss the observed isotope effect on the vibronic activity in the phosphorescence spectrum of PBQ-h_4 and conclude that the triplet state geometry is isotope dependent.

Section 4 is concerned with the isotope and external heavy atom effect on the ZFS parameter D of the lowest triplet state in PBQ-h_4 and it is shown that spin–orbit coupling effects are crucial in this matter.

The dynamics of energy migration in the PBQ-h_4 in PBQ-d_4 isotopic mixed crystal is dealt with in section 5 and it is suggested that exciton band–trap communication effects play an important role in the relaxation process among the spin substates of the PBQ-h_4 trap.

In section 6 experimental details are given and finally in section 7 all results are summarized and discussed in reference to a vibronic and electronic two-state model.

2. Singlet–triplet absorption spectra

2.1. Pure crystals

The basic problem in the understanding of the pure crystal singlet–triplet absorption spectra of PBQ-h_4 and -d_4 concerns the understanding of a Stark induced line 16.9 cm^{-1} (h_4) and 12.1 cm^{-1} (d_4) below the low-

est observed transition in the pure crystals. Our previous understanding of these features was based upon a model in which the lowest excited triplet state in PBQ-h_4 and -d_4 was thought to be dynamically distorted along b_{1u} type nuclear motions [5]. In this double minimum potential (DMP) model (fig. 2) of the lowest excited triplet state, the Stark induced absorption was assigned as the g-inversion level of this well, while the lowest observed transition in the pure PBQ-h_4 and -d_4 crystals was interpreted as the vibronically induced u-inversion level of this well. This DMP model seemed also quite satisfactory in explaining similar spectral features in the region of the lowest singlet $n\pi^*$ absorption [5]. In a recent paper on the assignments of the $n\pi^*$ singlet states in *p*-benzoquinone Dunn and Francis [7] however explained these spectral features as being caused by a near degeneracy (3.5 cm^{-1} splitting in PBQ-h_4!) of the B_{1g} and A_u $n\pi^*$ singlet states.

It therefore seems worthwhile to further investigate the applicability of the DMP model for the explanation of the lowest triplet state absorption region. In this section we will present and discuss the results of an isotope effect study on the oscillator strength and splitting of the "inversion" levels of the lowest triplet state in PBQ-h_4.

We were particularly interested in the isotope effect on the vibronic origin (u-inversion level) to probe the coupling mechanism between the B_{1g} and A_u $n\pi^*$ triplet state. Asymmetric isotopic substitution of course destroys inversion symmetry and results in the observation of the origin of the lowest $n\pi^*$ triplet state. This is illustrated in fig. 3 where the singlet–triplet absorption spectra of PBQ-h_4, -dh_3 and -2,6-d_2h_2 in the region of the origin of the g-type $n\pi^*$ state, are compared. Another consequence of the loss of inversion symmetry in the asymmetric *p*-benzoquinones is the observation of linear Stark effects both in absorption and emission of these species.

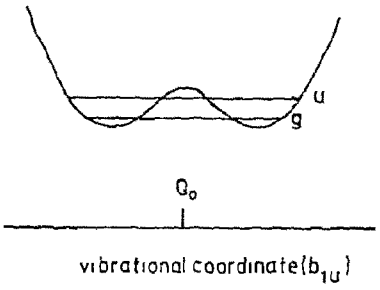

Fig. 2. Potential energy function along a b_{1u} normal coordinate of the lowest excited B_{1g} ($n\pi^*$) triplet state in PBQ-h_4. The inversion levels of this double minimum potential (DMP) well are split by 16.9 cm^{-1} in pure PBQ-h_4 crystals and only the u-inversion level is accessible by optical excitation from the groundstate configuration (Q_0).

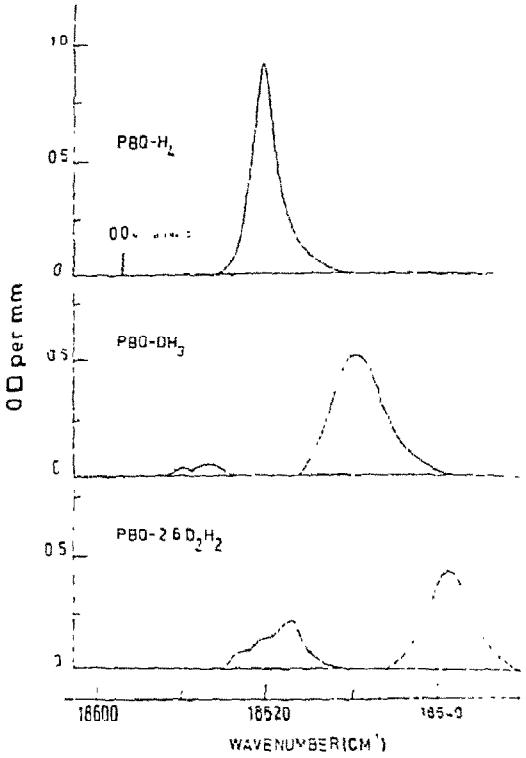

Fig. 3. *b*-polarized (incoming light perpendicular to the (20$\bar{1}$) cleavage plane) singlet–triplet absorption spectra of pure PBQ-h_4, PBQ-dh_3 and PBQ-2, 6-d_2h_2 crystals at 1.8 K. The origin of the lowest $n\pi^*$ triplet state is not observed in the case of PBQ-h_4 but its position has been deduced from Stark modulation experiments [5]. Note that optical density (OD) in this figure is defined as $\ln I_0/I$.

In table 1 we have gathered the results of our isotope effect study on the position and intensity of the "inversion" levels. Before discussing the data of table 1 we should mention one additional point: in disagreement with Trommsdorff [9] we find that the transition moment to the lowest $n\pi^*$ transition in toluquinone points along the oxygen–oxygen direction. Trommsdorff reported a deviation of the transition moment of this direction of 9°.

Table 1
Positions and integrated oscillator strength ($\times 10^9$ ln 10) of bands in the origin region of the lowest singlet–triplet transition of (isotopically) substituted *p*-benzoquinones at 1.8 K

Species	Line position (cm^{-1}) and integrated oscillator strength a) (in parentheses times 10^9 ln 10; ± 5%)				Averaged inversion splitting (cm^{-1})
PBQ-h_4	18602.8 (0);	18619.7 (6.8)			16.9
PBQ-dh_3	18609 (0.17);	18613 (0.25);	18630 (6.2)		19.0
PBQ-2,6-d_2h_2	18617 (0.5);	18620 (0.7);	18623 (1.4);	18641.4 (5.9)	21.4
PBQ-d_4	18649.2 (0);	18661.3 (7.5)			12.1
PBQ-h_3CH_3	18690 (12.7)				
PBQ-d_3CH_3	18732.8 (15.0)				

a) The integrated oscillator strength (f) has been calculated using the following expression:

$$f = \frac{1}{3} \times 4.31 \times 10^{-9} \int (\epsilon_{\parallel b} + \epsilon_{\perp b}) d\nu.$$

Returning now to the data of table 1 three things are noted:

(1) The total oscillator strength of the absorptions in the lowest singlet–triplet origin region of all PBQ isotopes is almost constant.

(2) The intensity of the energetically lowest observed line increases dramatically with an increase in perturbent. In the case of toluquinone (PBQ-CH_3) this has resulted in the appearance of only one absorption line in the origin region with twice the integrated oscillator strength compared to the PBQ-h_4 origin region.

(3) In the asymmetric PBQ isotopes the "inversion" splitting is significantly larger than in the symmetric ones.

Of the results summarized here only the first one seems difficult to explain on the basis of a DMP model for the lowest excited triplet state in PBQ-h_4.

An essential point of this model is the assumption that the u-inversion level is induced by vibronic coupling between the B_{1g} and A_u $n\pi^*$ triplet states. The u-inversion level thus acts as a "false origin" in the singlet–triplet absorption spectrum of the lowest B_{1g} ($n\pi^*$) triplet state. The data in table 1 now show this vibronic coupling process to be almost insensitive to deuteration. This is difficult to understand, especially in view of the observed large isotope effects on the (vibronically induced) phosphorescence spectrum of PBQ-h_4 discussed in section 3. It is shown in section 3 that the activity of the b_{1u} modes (promoting modes for the vibronic coupling between the B_{1g} and A_u $n\pi^*$ states) in the phosphorescence spectrum of PBQ-h_4 decreases dramatically on deuteration. In line with this observation we also expected the u-inversion level oscillator strength to be quite sensitive to deuteration, but as table 1 shows it is not. The u-inversion level thus behaves in absorption as an electronic and not as a vibronic state. On the other hand we will also show in section 3 that in the asymmetrically deuterated PBQs the induced origin (corresponding with the g-inversion level in PBQ-h_4) behaves as a vibronic induced level of b_{1u} symmetry. We will leave this controversial matter rest for a moment and return to it in sections 3 and 7. The other observations summarized above can be more easily explained on basis of a DMP model for the lowest triplet state in PBQ-h_4. The toluquinone origin region of the singlet–triplet absorption spectrum in this model is explained as the extreme case whereby the DMP well has been destroyed by the molecular asymmetric field. Absorption now takes place to a displaced potential well in the excited state and the origin oscillator strength is induced by direct spin–orbit coupling. The upper state displacement is confirmed by the measured dipole moment change on excitation ($\Delta\mu = 1.3 \pm 0.1$ D; $E_{eff} = 1.6\ E_{appl.}$) to the lowest $n\pi^*$ triplet state in toluquinone. The observed increased "inversion splitting" in the asymmetrically substituted PBQ isotopes of course can be explained in either an electronic or vibronic two-state model.

The conclusion of this section must be that the observed isotope effects on the absorption spectra give no unambiguous support to the previously proposed [5] DMP model for the lowest excited triplet state in PBQ-h_4.

2.2. Isotopic mixed crystals

In the previous section we have seen that small molecular perturbations have a drastic effect on the intensity of the origin of the lowest $n\pi^*$ triplet state in PBQ-h_4. In this section we will show that the effect of an asymmetric environment on this state is quite similar. The asymmetric environment in which we have studied PBQ-h_4, is the heavily doped isotopic mixed crystal. We have made a preliminary optical absorption, emission and EPR study of proto–deutero isotopic mixed crystals of PBQ throughout the whole concentration range. In this section we will only discuss the results obtained from the absorption study of which preliminary results have been given elsewhere [10]. Fig. 4 shows the absorption spectra of two heavily doped PBQ-h_4 in PBQ-d_4 isotopic mixed crystals. The upper one shows the spectrum of a crystal containing 24 mol % PBQ-h_4 while the lower one contains a similar mol % PBQ-d_4. The interesting point of these spectra is that they show "cluster state" absorptions in the gap between the absorptions of the pure PBQ-h_4 and PBQ-d_4 crystals. This indicates that these "cluster" states do not expose exciton band width features but are removed from the exciton band by static forces. Table 2 gives the results of an analysis of the spectra shown in fig. 4.

Our results of the isotopic mixed crystal absorption study can be summarized as follows:

(1) The u-inversion monomer level of PBQ-h_4 in a PBQ-d_4 crystal shifts 10.3 cm^{-1} to higher energy with respect to the pure proto crystal.

(2) The u-inversion monomer level of PBQ-d_4 in a PBQ-h_4 crystal shifts 11.1 cm^{-1} to lower energy with respect to the pure deutero crystal.

(3) "Cluster" absorptions show only minor shifts, but a significant change in intensity as a function of the relative proto–deutero concentration.

From these data we conclude that the pure crystal deuteration gap of 42 cm^{-1} (of the u-inversion levels) is partly (~ 11 cm^{-1}) due to a change in static forces upon deuteration. This static interaction apparently is very short range as only monomer and one sort of "dimer" and "trimer" states are observed outside the pure crystal exciton band. So far we have not discussed the nature of the local static interaction that

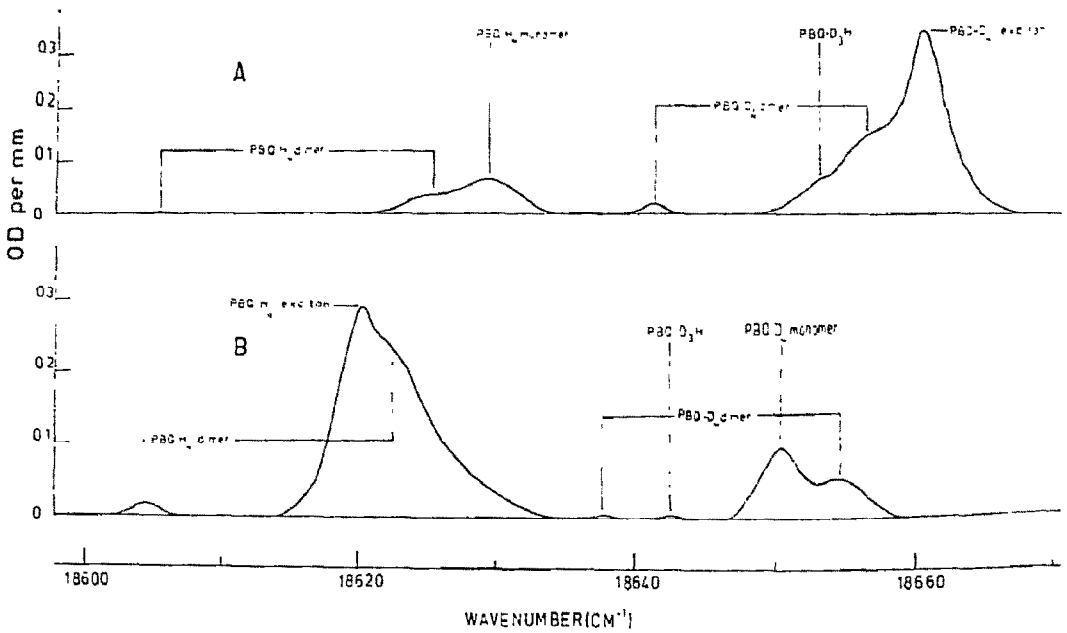

Fig. 4. Unpolarized heavily doped isotopic mixed crystal absorption spectra of PBQ-h_4 in PBQ-d_4 at 1.8 K. The spectra were taken with the incoming light perpendicular to the cleavage (20$\bar{1}$) plane. The upper spectrum (A) contains 24 mol % PBQ-h_4 and the lower one (B) contains a similar mol percentage of PBQ-d_4. Note that optical density (OD) in this figure is defined as $\ln I_0/I$.

Table 2
Line positions and analysis of singlet–triplet absorptions in isotopic mixed crystals of PBQ-h_4 in PBQ-d_4 at 1.8 K

Line position (cm^{-1}; ± 0.5 cm^{-1})	Analysis [a]	Line position (cm^{-1}; ± 0.5 cm^{-1})	Analysis
A: 24 mol % PBQ-h_4		B: 26 mol % PBQ-d_4	
18605.0	g'-level of PBQ-h_4 dimer	18604.3	g'-level of PBQ-h_4 dimer
18626.0	u'-level of PBQ-h_4 dimer	18620.5	"exciton" origin of u-level in PBQ-h_4
18630.0	u-level of PBQ-h_4 monomer	18623.0	u'-level of PBQ-h_4 dimer
18641.3	g'-level of PBQ-d_4 dimer	18638.5	g'-level of PBQ-d_4 dimer
18654.0	u'-level of PBQ-d_3h monomer	18642.6	u'-level of PBQ-d_3h monomer
18656.8	u'-level of PBQ-d_4 dimer	18650.3	u-level of PBQ-d_4 monomer
18660.9	"exciton" origin of u-level in PBQ-d_4	18654.3	u'-level of PBQ-d_4 dimer

[a] The prime on the g and u symmetry labels is used for those species that do not possess site inversion symmetry.

causes the observed isotope effects. It almost seems evident that the isotope effects observed here are due to hydrogen (deuterium) bonding effects that shift the electronic excitation that is mainly centered on oxygen. From the appearance of an origin in the case of a "dimer" cluster, as shown in fig. 4, we conclude that these hydrogen bonding effects are most effective between translationally inequivalent molecules.

It is important to realize that such a "translationally inequivalent dimer" (fig. 5) does not have inversion symmetry; in fact one of the molecules in the "dimer" (no. 1 in fig. 5) absorbs 4.0 cm^{-1} to lower energy than the other (no. 2 in fig. 5).

In such a "dimer" cluster only one of the oxygens in the PBQ molecule is favoured and this leads to a loss of inversion symmetry in the no. 1 PBQ molecule, making the origin in absorption and emission of such a cluster allowed. In a "translationally inequivalent trimer" (the PBQ molecules numbered 1,2 and 3 in fig. 5) inversion symmetry is preserved and no origin in either absorption or emission of such a trimer is expected. This conclusion is in agreement with experiments (see also section 5.2 and fig. 12).

We are now in a position to also understand the splittings shown in fig. 3 of the electronic origins of the lowest $n\pi^*$ triplet states in pure crystals of PBQ-dh_3 and PBQ-2,6-d_2h_2. The crystals of these molecules are chemically disordered in the sense that the excitation energy of a particular molecule depends upon the positions of the hydrogens (deuteriums) of the neighbouring molecules. The intensities of the lines are not easily calculated. There is both a statistical factor that determines the grouping of the molecules and a crystal field effect on the transition moment to the lowest state that affects the intensities.

We have not tried to further unravel these effects. Finally, in closing this section, we would like to point out that the isotope shift effects reported here are in agreement with a hydrogen (deuterium) bonding model in which the hydrogen (deuterium) bond is weakened in the electronically excited state.

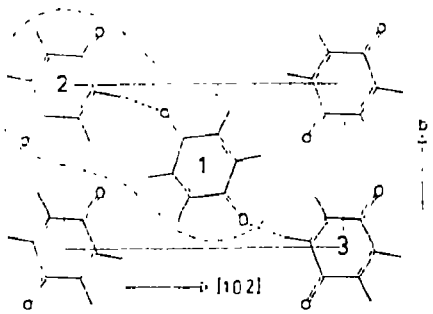

Fig. 5. Packing of the PBQ molecules as viewed perpendicular to the (20$\bar{1}$) cleavage plane [2]. Only molecules in one particular layer are shown here for clarity. The PBQ-h_4 molecules encircled (nr. 1 and nr. 2) form a PBQ-h_4 dimer (translational inequivalent) in a PBQ-d_4 host crystal. The hydrogen bonds, responsible for the cluster formations, are indicated by dotted lines. A PBQ-h_4 trimer in a PBQ-d_4 host lattice, as referred to in the text, is formed by the molecules numbered 1,2 and 3. Note that in this particular trimer inversion symmetry is preserved.

3. PBQ–mixed crystal phosphorescence spectra

3.1. Survey of the spectra

In this section we will discuss the phosphorescence spectra of the following *p*-benzoquinones: PBQ-h_4, -dh_3, -2,6-d_2h_2 and -CH_3 in isotopic mixed crystals.

The first isotopic mixed crystal study of PBQ-h_4 in PBQ-d_4 was made by Klump [11]. However, Klump analyzed the emission spectrum as arising from a crystal field induced B_{1u} ($\pi\pi^*$) triplet state and in order to achieve consistency in the vibrational analysis placed the origin of the emitting B_{1u} ($\pi\pi^*$) triplet state at 18638 cm^{-1}. A second isotopic mixed crystal study was made by Francis [12] who suggested the lowest emitting state in PBQ-h_4 to be of $^3B_{1g}$ ($n\pi^*$) symmetry with the observed origin in the PBQ-d_4 mixed crystal at 18605.5 cm^{-1}.

The absorption and emission experiments on isotopic mixed crystals, discussed in section 2.2, however show that the emission line at 18605.5 cm^{-1} is not a "PBQ-h_4 monomer" but a "PBQ-h_4 dimer" origin. The first *reported* isotopic mixed crystal phosphorescence study of PBQ-h_4 in PBQ-d_4 was performed by Koyanagi et al. [13]. These authors also concluded from a vibrational analysis of the PBQ-h_4 phosphorescence spectrum that the emitting triplet state in PBQ-h_4 is a B_{1g} ($n\pi^*$) state and interpreted a line observed at 18624 cm^{-1} in the emission spectrum as the origin of the emitting state.

Recently reported results of ODMR experiments, by Veenvliet and Wiersma [8], on single vibronic lines of the phosphorescence spectrum of PBQ-h_4 in PBQ-d_4 confirmed the assignment of the lowest triplet state in PBQ-h_4 as a B_{1g} ($n\pi^*$) state. These authors established the unobserved origin of the emitting state of PBQ-h_4 in PBQ-d_4 at 18613 cm^{-1}, thereby assuming that the inversion splitting in the pure and isotopic mixed crystals was the same. We will not further question the assignment of the lowest triplet state in PBQ-h_4 but instead concentrate on the vibrational analysis of the phosphorescence spectrum of PBQ-h_4 as a trap in PBQ-d_4. It will also be shown that all previous reports [8,11–13] of the "origin" position of PBQ-h_4 in a PBQ-d_4 crystal are wrong. The "true" origin of the emitting state of a PBQ-h_4 monomer in a PBQ-d_4 crystal will be shown to be located at 18609 ± 1 cm^{-1}. Fig. 6 shows the unpolarized emission spectrum of a 1 mol % PBQ-h_4 isotopic mixed crystal at 1.8 and 4.2 K.

In table 3 the positions and vibrational assignments of all the lines (except some weak features) in the phosphorescence spectrum of this isotopic mixed crystal are given. Table 3 also includes the final results of ODMR experiments performed on single vibronic lines in the phosphorescence spectrum of PBQ-h_4. Especially these experiments make the vibrational assignments unambiguous.

The vibrational analysis of the phosphorescence spectrum presented here is, on several occasions, substantially different from the one given by Koyanagi et al. [13]. This is mainly due to the fact that Koyanagi et al. [13] made a different (wrong) choice of origin position of the emitting state. The problem with the location of the origin of the triplet state of PBQ-h_4 in a PBQ-d_4 crystal is, that it is not observed and thus can be located only by indirect means. A further discussion of this problem is given in section 3.3.

In the asymmetrically substituted quinones the origin of the emitting state is observed and this makes the analysis of these spectra somewhat easier. Fig. 7 shows the phosphorescence spectra of PBQ-dh_3, -2,6-d_2h_2 and -CH_3 in isotopic mixed crystals at 1.8 K. The analysis of these spectra is given in tables 4–6.

A common feature of all quinones studied here is that the emission is heavily phonon assisted. In fig. 8 the emission spectra of PBQ-h_4 and PBQ-d_4 in a *p*-dibromo benzene (DBB) host crystal are given and this figure shows that the phonon assisted emission is not a peculiarity of the PBQ-d_4 host crystal. In fact, the emission spectra show that most of the integrated intensity is found in the phonon side bands. The electron–phonon coupling in these mixed crystals is thus a very competitive mechanism compared to higher order spin–orbit coupling effects in inducing the spin-space forbidden $^1A_g \leftarrow {}^3B_{1g}$ ($n\pi^*$) transition. We will not discuss these lattice features any further here and restrict ourselves to a discussion of the sharp molecular structure in the phosphorescence spectra of the quinones. Before proceeding with a discussion about the nature of the vibrations that appear in the emission spectra and the observed isotope effects it seems worthwhile to first find out what theory would predict for the vibronic activity in the emission spectrum of a B_{1g} ($n\pi^*$) triplet state.

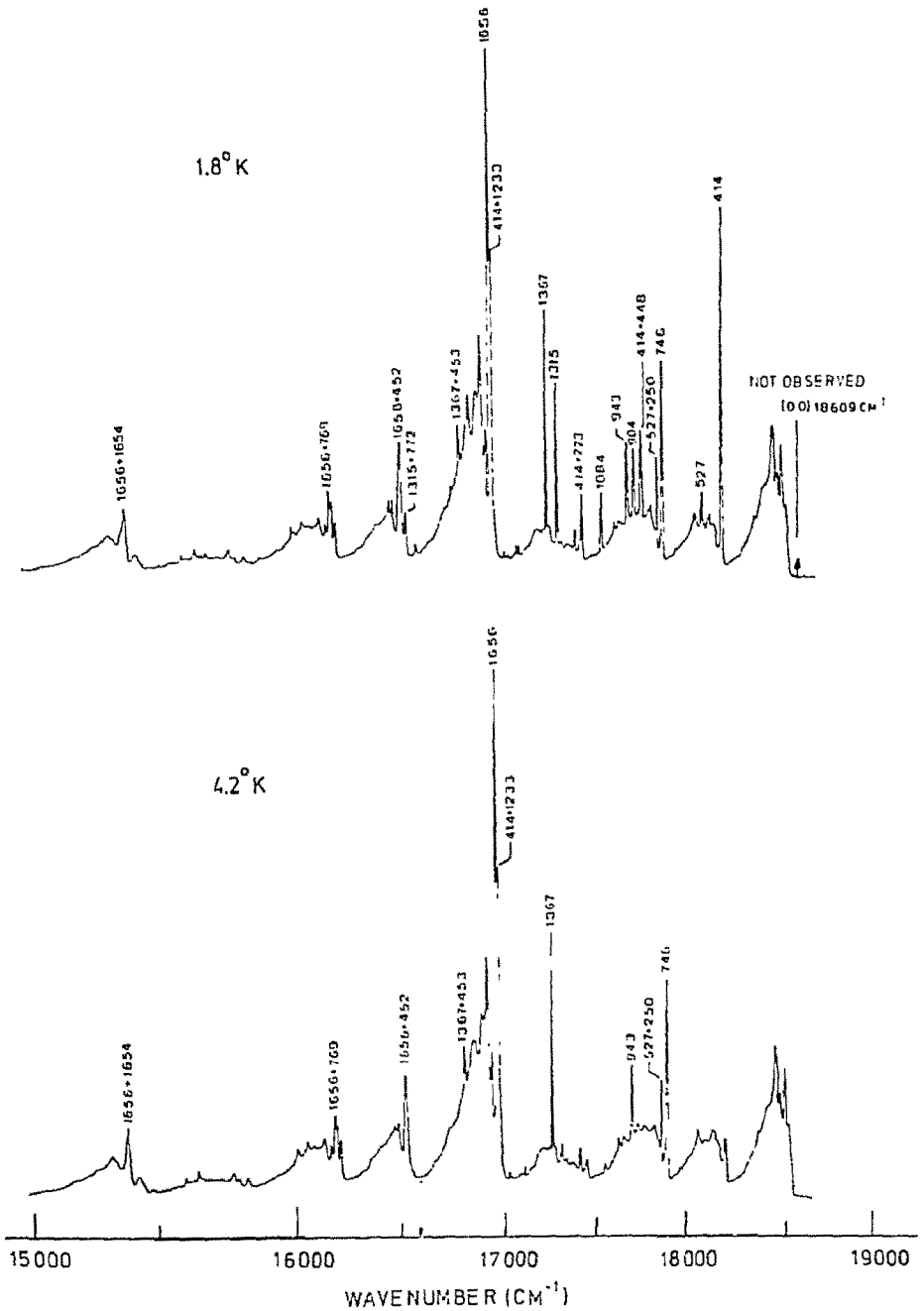

Fig. 6. Unpolarized phosphorescence spectrum taken from the cleavage $(20\bar{1})$ plane of a 1 mol % PBQ-h_4 in PBQ-d_4 isotopic mixed crystal at 1.8 and 4.2 K. Polarization measurements on this mixed crystal system however have shown that all the emission lines are completely long axis (z) polarized. The vibrational analysis of the 1.8 K spectrum is given in table 3.

Table 3. Vibrational analysis of and microwave effect on the phosphorescence spectrum of PBQ-h_4 as guest (1 mol %) in PBQ-d_4 at 1.8 K [$L = z(B_{1u})$; $M = y(B_{2u})$]

Position (vac cm^{-1}; ± 1 cm^{-1})	Separation from origin (cm^{-1})	Analysis [a]	Microwave effect (% ± 2%)	
			1936 MHz	2164 MHz
18609	0	origin, not observed [b]		
18581	28	lattice		
18557	52	lattice		
18539	70	lattice	+ 30	+ 12
18516	93	lattice		
18489	120	lattice	+ 30	+ 12
18195	414	(ν_{21}, b_{2u})	− 18	none
18082	527	(ν_{25}, b_{3u})	none	− 4
17863	746	(ν_{16}, b_{1u})	+ 41	+ 15
17832	777	527 + 250 (ν_{30}, b_{2g})	+ 41	+ 15
17747	862	414 + 448 (ν_6, a_g)	− 2	none
17705	904	(ν_{24}, b_{3u})	none	− 9
17666	943	(ν_{15}, b_{1u})	+ 26	+ 12
17525	1084	(ν_{20}, b_{2u})	− 6	none
17422	1187	414 + 773 (ν_5, a_g)	− 7	none
17294	1315	(ν_{19}, b_{2u})	− 7	none
17242	1367	(ν_{14}, b_{1u})	+ 25	+ 12
17221	1388	943 + 445 (ν_6, a_g)		
17091	1518	746 + 772 (ν_5, a_g)		
17076	1533	1084 + 449 (ν_6, a_g)		
17033	1576	b_{2u} or b_{3u} total symmetry		
17015	1594	b_{1u} total symmetry		
16962	1647	414 + 1233 (ν_9, b_{3g})	+ 41	+ 12
16953	1656	(ν_{13}, b_{1u})	+ 41	+ 12
16927	1682	1084 + 598 (ν_{10}, b_{3g})?		
16903	1706	943 + 763 (ν_5, a_g)		
16838	1771	1315 + 456 (ν_6, a_g)		
16789	1820	1367 + 453 (ν_6, a_g)		
16579	2030	b_{2u} or b_{3u} total symmetry		
16530	2079	414 + 1665 (ν_2, a_g)		
16522	2087	1315 + 772 (ν_5, a_g)		
16501	2108	1656 + 452 (ν_6, a_g)	+ 41	+ 12
16467	2142	1367 + 775 (ν_5, a_g)		
16452	2157	1388 + 769 (ν_5, a_g)		
16201	2408	746 + 1662 (ν_2, a_g)		
16184	2425	1656 + 769 (ν_5, a_g)	+ 41	+ 12
16177	2432	777 + 1655 (ν_2, a_g)		
16129	2480	1706 + 774 (ν_5, a_g)		
16005	2604	943 + 1661 (ν_2, a_g)		
15788	2821	b_{1u} total symmetry		
15754	2855	2079 + 776 (ν_5, a_g)		
15731	2878	2425 − 453 (ν_6, a_g)		
15726	2883	b_{1u} total symmetry		
15628	2981	1315 + 1666 (ν_2, a_g)		
15583	3026	1367 + 1659 (ν_2, a_g)		
15531	3078	(ν_{12}, b_{1u})?		
15346	3263	b_{1u} total symmetry		
15299	3310	1656 + 1654 (ν_2, a_g)	+ 41	+ 12

[a] The total symmetry of the modes is obtained from either ODMR experiments (column 4 and 5) or the temperature dependence of the phosphorescence spectrum (fig. 6). The numbering and final identification of the normal modes was made by comparison with the ones obtained by Dunn and Francis [17] from an infrared and Raman study of pure PBQ-h_4 crystals.

[b] The origin position is deduced from isotopic mixed crystal absorption experiments (section 3.3). Alternatively the measured phonon frequencies in the phosphorescence spectra of PBQ-dh_3 and PBQ-2,6-d_2h_2 in a PBQ-d_4 host crystal (tables 4 and 5) can be used to extrapolate back to the origin of the lowest triplet state of PBQ-h_4 in a PBQ-d_4 mixed crystal.

3.2. Theoretical considerations

In a centrosymmetric molecule like *p*-benzoquinone-h_4 direct spin–orbit coupling cannot be responsible for mixing the B_{1g} ($n\pi^*$) triplet state with electric dipole allowed singlet states. The observed absorptive and emissive transition moment to and from this state must then be caused by perturbations that invoke deformations of the molecule away from the equilibrium geometry.

Orlandi and Siebrand [15] have shown that an elegant description of such effects can be given using a perturbation scheme that partitions the total hamiltonian as follows:

$$H_M = H_M^0 + H_M^1. \tag{1}$$

The eigenfunctions of H_M^0 are the pure spin adiabatic Born–Oppenheimer functions

$$\psi_{mv}(q, Q) = \phi_m(q, Q)\,\chi_{mv}(Q), \tag{2}$$

and H_M^1 includes the terms $T_N + H_{SO}$.

In this perturbation scheme the first term that goes beyond the Condon approximation in dealing with H_{SO} is the so called spin-forbidden Herzberg–Teller induced component of the (electric dipole allowed) transition moment. This component can be written as follows:

$$\sum_i \Bigg\{ (E_i - E_n)^{-1} \left[\langle {}^\mu\phi_m | p | {}^\mu\phi_i \rangle \left(\frac{\partial}{\partial Q} \langle {}^\mu\phi_i | H_{SO} | {}^\nu\phi_n \rangle \right) + \left(\frac{\partial}{\partial Q} \langle {}^\mu\phi_m | p | {}^\mu\phi_i \rangle \right) \langle {}^\mu\phi_i | H_{SO} | {}^\nu\phi_n \rangle \right]_{Q_0} + (E_i - E_m)^{-1} \left[\langle {}^\mu\phi_m | H_{SO} | {}^\nu\phi_i \rangle \left(\frac{\partial}{\partial Q} \langle {}^\nu\phi_i | p | {}^\nu\phi_n \rangle \right) + \left(\frac{\partial}{\partial Q} \langle {}^\mu\phi_m | H_{SO} | {}^\nu\phi_i \rangle \right) \langle {}^\nu\phi_i | p | {}^\nu\phi_n \rangle \right]_{Q_0} \Bigg\} \times \langle X_{mv} | Q - Q_0 | X_{nw} \rangle. \tag{3}$$

There is a second, the so called spin-forbidden Born–Oppenheimer induced component to the transition moment that in this perturbation treatment appears in the same order and therefore, in principle, should be dealt with on equal footing [15].

We will not explicitly formulate this term here but merely state that, as far as vibronic selection rules are concerned, this term leads to no new effects. The first thing that emerges from a closer look at eq. (3) is that all four terms lead to the same selection rules and further that it seems impossible to disregard certain terms off hand.

To examine the different "coupling routes" in more detail we expand, e.g., the electronic Q-dependent part of the first term in eq. (3) as follows:

$$\frac{\partial}{\partial Q} \langle {}^\mu\phi_i | H_{SO} | {}^\nu\phi_n \rangle = \sum_j \Big\{ - \langle {}^\mu\phi_i | \partial/\partial Q | {}^\mu\phi_j \rangle \langle {}^\mu\phi_j | H_{SO} | {}^\nu\phi_n \rangle + \langle {}^\mu\phi_i | H_{SO} | {}^\nu\phi_j \rangle \langle {}^\nu\phi_j | \partial/\partial Q | {}^\nu\phi_n \rangle \Big\} + \langle {}^\mu\phi_i | \partial H_{SO}/\partial Q | {}^\nu\phi_n \rangle. \tag{4}$$

We are now in a position to more specifically discuss the case of *p*-benzoquinone and therefore make the following identifications: ${}^\nu\phi_n = {}^3B_{1g}(n\pi^*)$; ${}^\mu\phi_m = {}^1A_g$ (ground state) and ${}^\mu\phi_i = {}^1B_{1u}(\pi\pi^*)$. The latter identification is based upon the notion that the phosphorescence spectrum of PBQ is completely long axis ($L = z$) polarized. We further use the well-known fact that in azines and ketones [16] the one center spin–orbit coupling terms completely dominate a spin–orbit coupling calculation. This means that in the case of *p*-benzoquinone the spin–orbit coupling terms at oxygen only need be considered. The first term in eq. (4) therefore will only be effective in inducing electric dipole intensity in the z and y spin substates of the ${}^3B_{1g}$ ($n\pi^*$) state through those b_{1u} and b_{2u} in plane vibrations (ipv) that are active in the vibronic coupling between the pertinent singlet states. The second term involves vibronic coupling in the triplet manifold and subsequently spin–orbit coupling with the $B_{1u}(\pi\pi^*)$ singlet state. Again only ipv are expected to be activated and in the case of PBQ-h_4 specifically, the vibronic coupling between the B_{1g} and A_u $n\pi^*$ triplet states might be effective in inducing the z-spin substate through b_{1u} modes. The last term in eq. (4), the so called spin–orbit vibronic term deserves special attention. As spin–orbit coupling is only effective at

the oxygen atoms this term will only contribute significantly for those modes, of the proper symmetry, that have large amplitudes at the carbonyl oxygens. This term is therefore expected to induce intensity in all three z, y and x spin substates through mainly "carbonyl" motions of b_{1u}, b_{2u} and b_{3u} symmetry respectively. Asymmetric motions of the carbonyl oxygens thus lead to constructive interference of the spin–orbit coupling terms on oxygen that cancel in the *p*-benzoquinone equilibrium configuration.

The other terms in eq. (3) can be dealt with in a similar fashion and yield comparable results, namely that the phosphorescence spectrum of the B_{1g} ($n\pi^*$) triplet state of PBQ-h_4 will be induced by modes of b_{1u}, b_{2u} and b_{3u} symmetry.

So far we have ignored the contribution of spin-forbidden Born–Oppenheimer effects to the induced transition moment. Orlandi and Siebrand [15] have shown that in general the contribution of Herzberg–Teller and Born–Oppenheimer vibronic effects to the total transition moment will interfere and that these "mechanisms" only can be distinguished by their isotope effects. In sections 3.4 and 4.2 we will show that the observed isotope effects on the vibronic activity in the phosphorescence spectrum of PBQ-h_4 probably are not due to a change in vibrational overlap but most likely are caused by the fact that the excited state structure is sensitive to isotopic substitution.

3.3. Vibrational analysis of the phosphorescence spectrum of PBQ-h_4

We will now return to a discussion of the vibrational analysis and activity observed in the phosphorescence spectra of the *p*-benzoquinones. Of prime concern in any vibrational analysis of an emission spectrum is an accurate knowledge of the origin position of the emitting state. In the PBQ-d_4 crystal a center of inversion at the molecular site is preserved [2] and we therefore do not expect nor observe an origin in the emission spectrum of the $^3B_{1g}$ ($n\pi^*$) state of PBQ-h_4 in this host crystal. The origin of the phosphorescence spectrum of PBQ-h_4 in a PBQ-d_4 crystal was located through an analysis of the absorption and emission spectra of isotopic mixed crystals. In section 2.2 we showed that in case of a translationally inequivalent (ti) dimer the origin of the $^3B_{1g}$ ($n\pi^*$) state is induced. We have located the origin of such a PBQ-h_4 dimer in the phosphorescence spectrum of a 5 mol % PBQ-h_4 in PBQ-d_4 isotopic mixed crystal at 18605.0 cm^{-1}. The singlet–triplet absorption spectra of a heavily doped isotopic mixed crystal shows (fig. 4) that the u-inversion level monomer–ti dimer shift is 4.0 cm^{-1}. Assuming the same shift for the g-inversion levels of these species one locates the origin of the B_{1g} ($n\pi^*$) triplet state of a PBQ-h_4 monomer in a PBQ-d_4 mixed crystal at 18609 ± 1 cm^{-1} †. A vibrational analysis of the phosphorescence spectrum of PBQ-h_4 based upon this origin yields values for the frequencies of the fundamentals that are in excellent agreement with the ones obtained by Dunn and Francis [17] from an analysis of the infrared and Raman spectra of solid PBQ-h_4.

We therefore feel quite certain about the origin position although it would be worthwhile to have this confirmed by means of a heat-pulse [18] modulated phosphorescence spectrum of the PBQ mixed crystal system. The question remains why the origin position of 18613 cm^{-1} proposed previously [8] apparently is wrong. This origin position was deduced from the observed Stark effect on pure PBQ crystals [5] and the u-inversion monomer level shift in isotopic mixed crystals. Our preliminary conclusion is that either the inversion splitting in the pure and isotopic mixed crystals is different or that the triplet exciton-bandwidth of the lowest B_{1g} ($n\pi^*$) triplet state is at least 4 cm^{-1}. This point certainly deserves further investigation.

The vibrational analysis of the phosphorescence spectrum of PBQ-h_4 in PBQ-d_4 based upon an origin at 18609 cm^{-1} is given in table 3 and shows that all modes assigned, are of total b_{1u}, b_{2u} or b_{3u} symmetry in agreement with theoretical expectations. In fact the 1.8 K phosphorescence spectrum can be completely understood on the basis of three independently decaying z, y and x spin substates each emitting "exclusively" modes of total b_{1u}, b_{2u} and b_{3u} symmetry respectively. This also explains the 4.2 K emission spectrum as being caused by thermalization among the spin sublevels while the molecule now decays through the fastest (z) channel (see section 5.1). It is also possible to separate the b_{1u}, b_{2u} and b_{3u} modes by time resolving the emission spectrum, as we have done,

† Recently performed Stark-modulation experiments on the phosphorescence of PBQ-h_4 in PBQ-d_4 at 1.8 K directly locate the (monomer) origin of the emission spectrum at 18610.2 ± 0.5 cm^{-1} in good agreement with the number reported here.

but in this case there is no additional information that can be obtained from such an experiment.

We will now discuss the vibronic activity in the phosphorescence spectrum of PBQ-h_4. The 4.2 K emission spectrum of fig. 6, containing only modes of total b_{1u} symmetry, shows the most intense line in the spectrum to be found at 1656 cm^{-1} from the origin and table 3 shows that we have assigned this line as the fundamental b_{1u} C=O stretching mode ν_{13}. Only 9 cm^{-1} to higher energy of ν_{13} another line is detected which was interpreted as the combination mode $\nu_{21} + \nu_9$.

Dunn and Francis [17] characterize ν_{21} as a b_{2u} C=O bending and ν_9 as a b_{3g} C–H bending mode. The intensity of the combination mode most likely is enhanced by Fermi resonance coupling with ν_{13}. This idea is supported by a study of the emission spectrum of PBQ-h_4-$^{18}O_2$ as guest in a PBQ-h_4 crystal. In this case the b_{1u} C=O stretching mode is a nice sharp single line in agreement with the fact that the combination mode $\nu_{21} + \nu_9$ in this case is 65 cm^{-1} higher in frequency than ν_{13} [19].

Other b_{1u} fundamentals in the phosphorescence spectrum are found at 746 cm^{-1} (ν_{16}, ring bending), 943 cm^{-1} (ν_{15}, C–C stretching) and 1367 cm^{-1} (ν_{14}, C–H bending). The only b_{1u} mode that we have not been able to identify in the spectrum is ν_{12}, a C–H stretching mode.

Another combination mode of total b_{1u} symmetry is detected at 777 cm^{-1} and assigned as $\nu_{25} + \nu_{30}$. These are both C=O bending modes of b_{3u} and b_{2g} symmetry respectively [17].

The rest of the stronger lines in the phosphorescence spectrum of PBQ-h_4 at 4.2 K can all be explained as combinations of these b_{1u} modes and totally symmetric ones of 452 cm^{-1} (ν_6, ring bending), 775 cm^{-1} (ν_5, C–C stretching) and 1660 cm^{-1} (ν_2, C=O stretching). At this point it is interesting to note that the same totally symmetric modes (ν_2, ν_5 and ν_6) are also found in the phosphorescence spectrum of the A_u ($n\pi^*$) triplet state of PBQ-h_4 in the gas phase [20]. The intensity distribution among these modes however is completely different. The emission spectrum from the ^3A_u ($n\pi^*$) state is completely dominated by a progression in the C=O stretching mode ν_2 and combinations of ν_2 with ν_5 and ν_6. The obvious conclusion is that in the ^3A_u ($n\pi^*$) state the C=O bonding distance is more changed on excitation than in the $^3B_{1g}$ ($n\pi^*$) state.

The larger displacement along the C=O stretching mode (ν_2) in the ^3A_u ($n\pi^*$) excited state strongly suggests that in this state the $n\pi^*$ excitation is more localized on the carbonyl functions than in the corresponding $^3B_{1g}$ ($n\pi^*$) state.

We will now return to the vibrational analysis of the phosphorescence spectrum arising from the $^3B_{1g}$ ($n\pi^*$) state of PBQ-h_4 and discuss the additional lines that appear in the 1.8 K emission spectrum. ODMR experiments on single vibronic lines of the phosphorescence spectrum at 1.8 K have shown that these additional lines are due to modes of total b_{2u} and b_{3u} symmetry. Table 3 shows that the following b_{2u} fundamentals can be identified in the phosphorescence spectrum: ν_{21}, a C=O bending mode at 414 cm^{-1}; ν_{20}, a C–H bending mode at 1084 cm^{-1}; and ν_{19}, a C–C stretching mode at 1315 cm^{-1}. The b_{2u} C–H stretching mode (ν_{17}) and C=C stretching mode (ν_{18}) are not found in the spectrum. Finally we report in table 3 observation of the b_{3u} modes ν_{25}, a C=O bending mode at 527 cm^{-1} and ν_{24}, a C–H out of plane bending mode at 904 cm^{-1} from the origin. In the isotopic mixed crystal we do not observe ν_{26}, a b_{3u} ring distortion mode, but this mode is observed in the phosphorescence spectrum of PBQ-h_4 when p-dibromobenzene is used as a host crystal (fig. 8).

The important question now is which "mechanisms" are responsible for the appearance of the vibronically induced spectrum. This paper is not aimed at answering that question in any detail but a few preliminary suggestions will be made. From the theoretical discussion described in section 3.2 it is clear that the C=O stretching and bending modes ν_{13} (b_{1u}), ν_{21} (b_{2u}) and ν_{25} (b_{3u}), having large amplitudes at the carbonyl oxygens, are expected to be induced through spin–orbit vibronic coupling as described, e.g., by the third term in eq. (4) The near degeneracy of the B_{1g} and A_u $n\pi$ triplet states however does not exclude the possibility that ν_{13} is also induced by Herzberg–Teller (second term in eq. (4)) or Born–Oppenheimer vibronic coupling effects.

The ring bending, C–C stretching and C–H bending modes observed in the spectrum are expected to be induced only by the vibronic coupling effects. A method that, in principle, discriminates between the HT and BO vibronic coupling effects is an isotope effect study on the vibronic activity [15].

This method assumes of course that the excited state structure does not change on isotopic substitu-

tion and that Duschinsky effects [21], due to normal coordinate mixing upon isotopic substitution, are negligible.

3.4. Isotope effect on the vibronic activity in the phosphorescence spectrum of PBQ-h_4

Fig. 7 shows the phosphorescence spectra of PBQ-dh_3, -2,6-d_2h_2 and -CH_3 in isotopic mixed crystals at 1.8 K, and tables 4–6 contain the analyses of these spectra. The change in the phosphorescence spectrum of PBQ-h_4 upon mono deuteration is very striking as can be seen in fig. 7. Besides the appearance of an electronic origin, which was expected (section 2.1) the splitting and collapse in intensity of the b_{1u} C=O stretching mode (ν_{13}) is amazing. (We assume here that it is legitimate to compare the b_{1u} vibronic intensity with the (b_{1u}) phonon induced intensity in the phosphorescence spectrum of PBQ and the latter is assumed to be independent of isotopic substitution.) The rest of the spectrum has also changed drastically, especially noteworthy in this regard is the complete collapse in intensity of the "b_{1u}" modes ν_{14} and ν_{15}.

Another point to be noted is the loss of intensity of the "b_{2u}" modes ν_{19} (C–C stretching) and ν_{20} (C–H bending) versus the intensity of the b_{2u} mode ν_{21} (C=O bending). We have also not been able to identify the "b_{3u}" mode ν_{24} (C–H out of plane bending) while the b_{3u} mode ν_{25} (C=O bending) is observed in the phosphorescence spectrum of PBQ-dh_3. In the phosphorescence spectrum of PBQ-2,6-d_2h_2 also shown in fig. 7 we observe similar large deuteration effects. The enormous decrease in intensity of the "b_{2u}" and "b_{3u}" modes however is not a molecular effect but is due to trap–exciton band communication effects as will be shown in section 5. It thus only is legitimate to compare relative intensities among modes of the same "symmetry". The origin intensity, versus the rest of the spectrum, is quite significant in the PBQ-2,6-d_2h_2 phosphorescence spectrum as fig. 7 shows, but this was of course in view of the singlet–triplet absorption spectrum of this molecule (section 2.1), to be expected. It thus seems clear that parity selection rules in this molecule no longer work. Especially the mixing of g and u modes of similar character may change the emission spectrum appreciable. As an example we mention

Table 4
Vibrational analysis of the phosphorescence spectrum of PBQ-dh_3 as guest (1 mol%) in PBQ-d_4 at 1.8 K

Position (vac cm^{-1}; ± 1 cm^{-1})	Separation from origin (cm^{-1})	Analysis [a)]
18620	0	origin
18572	48	lattice (shoulder)
18550	70	lattice (shoulder)
18527	93	lattice (shoulder)
18500	120	lattice (shoulder)
18207	413	ν_{21}
18122	498	ν_{25}
17899	721	ν_{16}
17876	744	498 + 246 (ν_{30})
17758	862	413 + 449 (ν_6)
17740	880	ν_{15}
17732	888	isotopic impurity?
17659	961	ν_{20}
17504	1116	
17442	1178	413 + 765 (ν_5)
17431	1189	744 + 445 (ν_6)
17327	1293	ν_{19}
17289	1331	ν_{14}
17281	1339	888 + 451 (ν_6)
17135	1485	721 + 764 (ν_5)
16972	1648	ν_{13}
16963	1657	ν_2
16523	2097	1648 + 449 (ν_6)
16515	2105	1657 + 448 (ν_6)
16205	2415	1648 + 767 (ν_5)
16195	2425	1657 + 768 (ν_5)
15318	3302	1648 + 1654 (ν_2)

a) The "total symmetry assignment" is primarily based on comparison of the phosphorescence spectrum of PBQ-dh_3 in PBQ-d_4 at 1.8 K with the emission spectrum of PBQ-dh_3 in DBB at 1.8 and 4.2 K. Modes that have drastically decreased in intensity at 4.2 K in the latter mixed crystal system have been assigned as modes of total "b_{2u}" or "b_{3u}" symmetry. The final vibrational analysis was made on basis of correlation with the PBQ-h_4 data (fig. 6 and table 3) and using the vibrational analysis of PBQ-dh_3 as reported by Becker et al. [19]. Some of our assignments however disagree with the latter report.

here the splitting of the C=O stretching mode in the phosphorescence spectrum of PBQ-2,6-d_2h_2. The stronger of the two lines is assigned as ν_{13} and the weaker one as ν_2, both being C=O stretching modes of a_1 symmetry in the C_{2v} symmetric PBQ-2,6-d_2h_2 molecule. These modes correlate with the b_{1u} (ν_{13}) and a_g(ν_2) C=O stretching modes in PBQ-h_4. Another

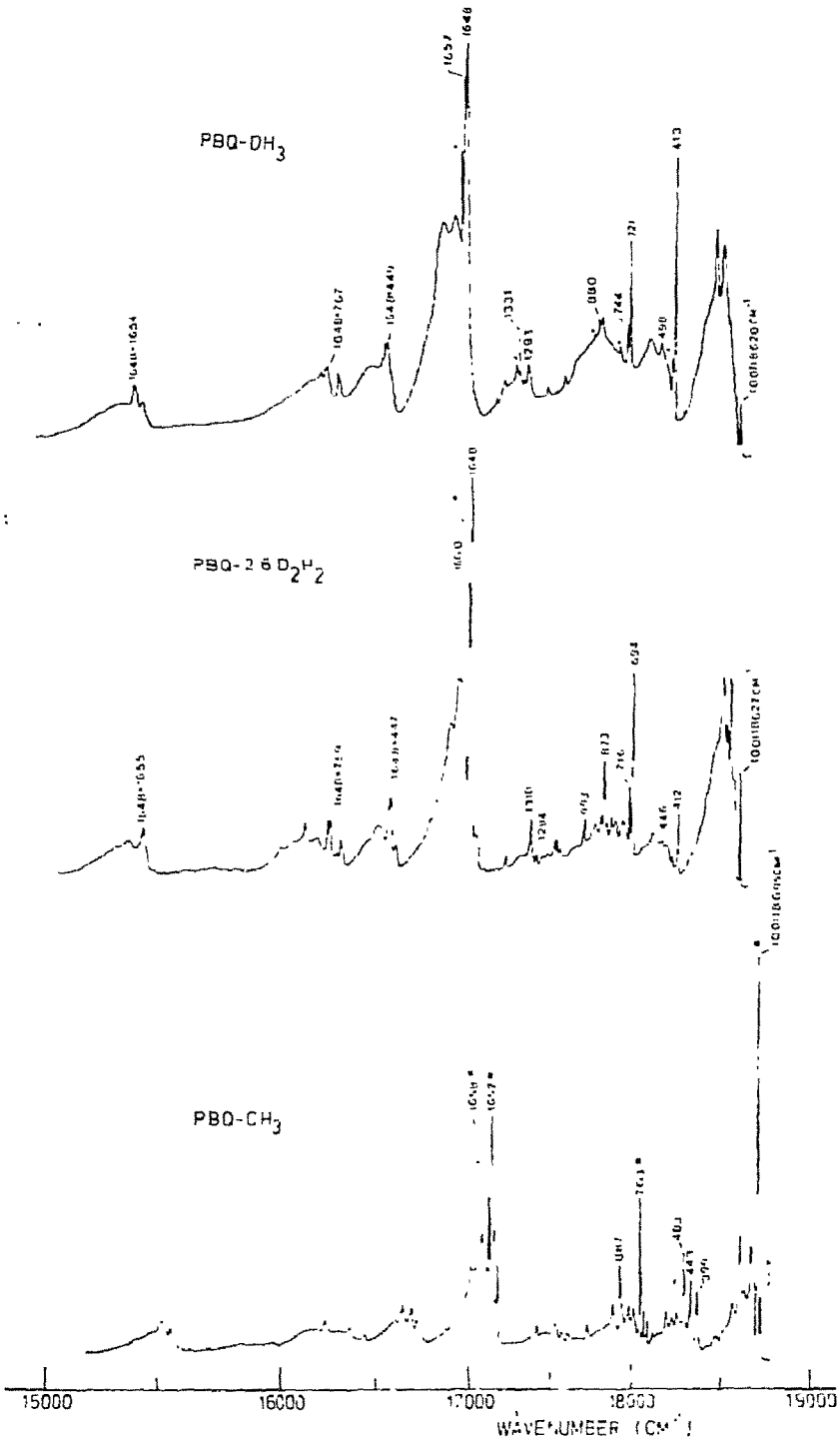

Fig. 7. Unpolarized phosphorescence spectra, taken from the cleavage planes at 1.8 K, from the following isotopic mixed crystal systems (all 1 mol % guest concentration): PBQ-dh_3 and PBQ-2,6-d_2h_2 in a PBQ-d_4 host crystal and PBQ-CH_3 (toluquinone) in a PBQ-d_3CH_3 isotopic mixed crystal. The lines marked with plus (+) signs in all spectra are due to isotopic impurity emission. Only the lines in the PBQ-CH_3 spectrum indicated by asterisks (*) have been positively identified, by means of ODMR experiments, as genuine PBQ-CH_3 emission.

Table 5
Vibrational analysis of the phosphorescence spectrum of PBQ-2,6-d_2h_2 as guest (1 mol %) in PBQ-d_4 at 1.8 K

Position (vac cm^{-1}; ± 1 cm^{-1})	Separation from origin (cm^{-1})	Analysis [a]
18627	0	origin
18586	41	lattice (shoulder)
18556	71	lattice (shoulder)
18532	95	lattice (shoulder)
18506	121	lattice (shoulder)
18215	412	ν_{21}
18181	446	ν_6
17933	694	ν_{16}
17911	716	$\nu_{25} + \nu_{30}$
17754	873	ν_{15}
17634	993	
17492	1135	694 + 441 (ν_6)
17469	1158	716 + 442 (ν_6)
17460	1167	412 + 755 (ν_5)
17355	1272	isotopic impurity (or ν_{19})
17333	1294	ν_{19} (or isotopic impurity)
17317	1310	ν_{14}
17175	1452	694 + 758 (ν_5)
16979	1648	ν_{13}
16967	1660	ν_2
16532	2095	1648 + 447 (ν_6)
16520	2107	1660 + 447 (ν_6)
16266	2361	694 + 1667 (ν_2)?
16220	2407	1648 + 759 (ν_5)
16208	2419	1660 + 759 (ν_5)
16093	2534	
15324	3303	1648 + 1655 (ν_2)

[a] See footnote table 4 and read instead of PBQ-dh_3 now PBQ-2,6-d_2h_2.

Table 6
Line positions of the stronger bands in the phosphorescence spectrum of PBQ-h_3CH_3 as guest (1 mol %) in PBQ-d_3CH_3 at 1.8 K

Position (vac cm^{-1}; ± 1 cm^{-1})	Separation from origin (cm^{-1})	Remarks [a] and preliminary analysis [b]
18705	−10	origin PBQ-dh_2CH_3 emission
18695	0	origin PBQ-h_3CH_3 emission
18296	399	
18252	443	
18212	483	ν_6?
17932	763	ν_{16}
17808	887	
17043	1652	ν_{13}
17037	1658	ν_2
16634	2061	399 + 1662 (ν_2)
16592	2103	443 + 1660 (ν_2)
16574	2121	
16357	2338	
16263	2432	
16155	2540	1652 + 888
15387	3308	1652 + 1656 (ν_2)

[a] ODMR experiments performed on this mixed crystal system show that at least the origin in the emission spectrum, a mode at 763 cm^{-1} and the modes at 1652 and 1658 cm^{-1} belong to the same emitting species. Further isotopic mixed crystal phosphorescence and ODMR studies on this mixed crystal system are in progress.

[b] We have also performed phosphorescence measurements on PBQ-CH_3 in DBB at 1.8 K. The analysis of the emission spectrum of PBQ-CH_3 in this host crystal however is complicated by the presence of impurity emission (photolysis products of PBQ-CH_3) in the same spectral region.

very important point to be noted from the phosphorescence spectrum of PBQ-2,6-d_2h_2 is that the appearance of an electronic origin is not accompanied by the appearance of an "allowed" part in the emission spectrum. Also the absence of overtones of totally symmetric modes shows that these modes (correlating with a_g and b_{1u} modes in PBQ-h_4) are still vibronically induced. In fact it looks as if the origin intensity itself is of vibronic character. This of course is expected on basis of the DMP model of the lowest triplet state in PBQ-h_4. In the C_{2v} symmetric PBQ-2,6-d_2h_2 molecule the vibronically induced u-inversion level is mixed with the lowest (emitting) g-inversion level. Absorption experiments have shown (section 2.1) that the total oscillator strength in this region is conserved and on basis of the DMP model one would then predict the electronic origin in the PBQ-2,6-d_2h_2 spectrum to be vibronically induced and to be of b_{1u} (a_1 in C_{2v}) character. Temperature dependent phosphorescence spectra of PBQ-2,6-d_2h_2 show the origin intensity indeed to be emitted from the z-spin substate of the molecule.

The phosphorescence spectrum of PBQ-CH_3 (toluquinone) in ring deuterated PBQ-CH_3 is also shown in fig. 7. The origin is now by far the most intense line in the emission spectrum. The emission has the appearance of an electronically allowed transition but considering the spectra of the other quinones, we suggest that part of the spectrum is still vibronically induced.

To complete the picture we have also studied the phosphorescence spectrum of PBQ-d_4 in a DBB host

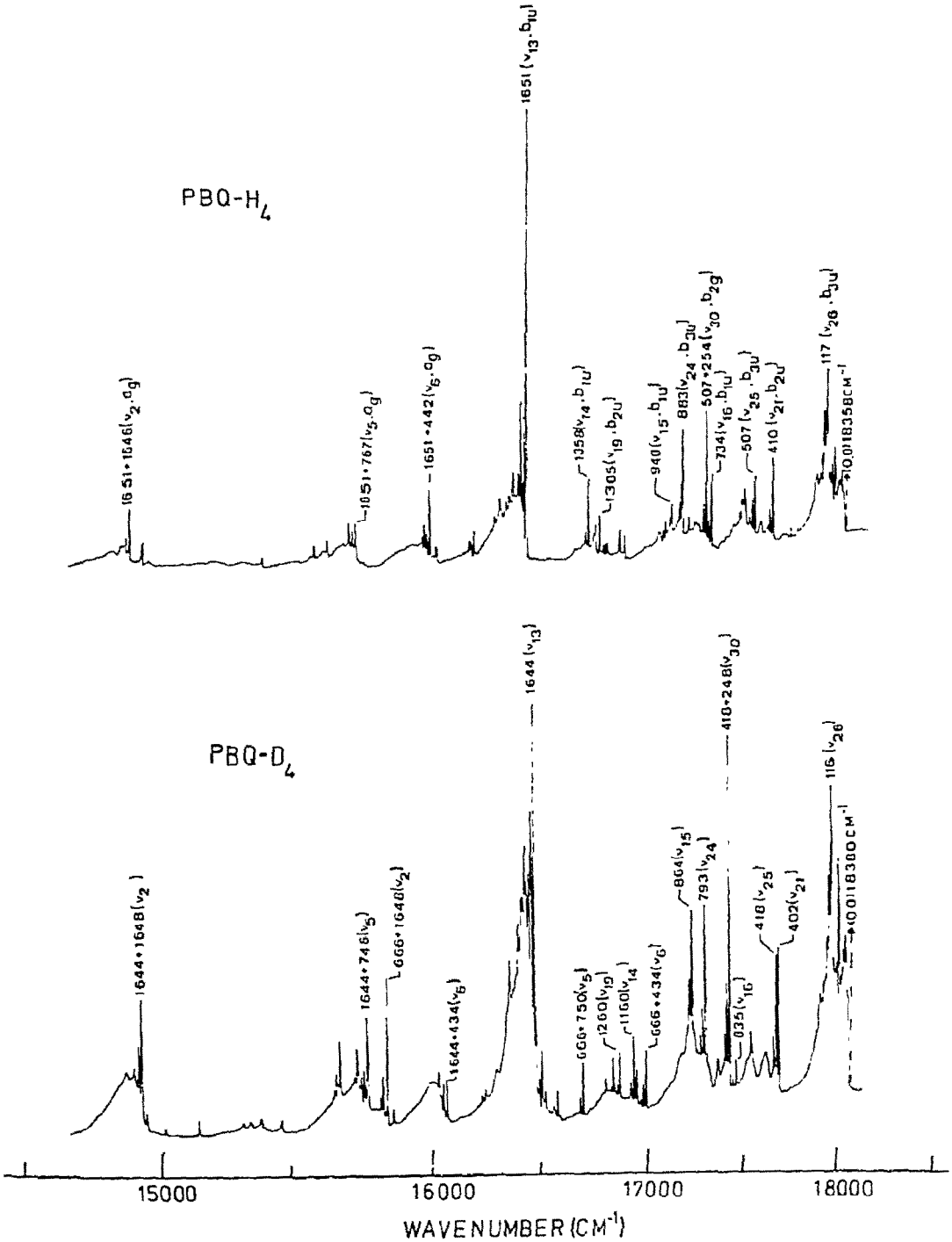

Fig. 8. Unpolarized phosphorescence spectra and vibrational analysis thereof of PBQ-h_4 (upper) and PBQ-d_4 (lower) as guest ($\lesssim$ 0.1 mol %) in a *p*-dibromobenzene (DBB) crystal at 1.8 K.

crystal. Fig. 8 shows this emission spectrum where we have, for comparison purposes, also included the phosphorescence spectrum of PBQ-h_4 in the same host crystal. The vibrational analysis of these spectra has been included in this figure as well.

Part of the vibrational analysis of the PBQ-h_4 emission spectrum in DBB was reported earlier by Attia et al. [14]. Comparison between figs. 6 and 8 shows that the phosphorescence spectrum of PBQ-h_4 in PBQ-d_4 and DBB is rather similar, except for the fact that the b_{1u} C=O stretching mode (ν_{13}) is twice and the b_{1u} combination mode $\nu_{25} + \nu_{30}$ (both C=O bending modes) is at least four times as intense, compared to the intensity of the other b_{1u}-modes, in the latter host crystal. ODMR experiments have shown (section 4) that the ZFS parameter $|D|$ of PBQ-h_4 in DBB is also significantly larger than in PBQ-d_4 and this suggests the $n\pi^*$ excited triplet state of PBQ-h_4 to be more localized on oxygen in a DBB than in a PBQ-d_4 host crystal. These effects are discussed in greater detail in section 4.3. Fig. 8 shows that the vibronic activity in the phosphorescence spectra of PBQ-h_4 and PBQ-d_4 is greatly different. Compared to the phonon-induced intensity (which again we assume to be independent of guest isotopic substitution) the b_{1u} C=O stretching mode (ν_{13}) has lost more than 2/3 of its original intensity in PBQ-d_4 and the same isotope effect is observed for the b_{1u} C–H bending mode ν_{14}. The b_{1u} C–C stretching mode ν_{15} however has tripled its intensity in PBQ-d_4. The activity of all b_{2u} and b_{3u} modes is also found to have decreased in PBQ-d_4 and we have measured an intensity reduction factor of 1.6 ± 0.1 for these modes. Comparison of the spectra in fig. 8 further shows that the intensity distribution among the totally symmetric modes ν_2, ν_5 and ν_6 based, e.g., on ν_{13} has also changed considerably.

In the case of PBQ-d_4 the intensity of $\nu_{13} + \nu_2$ is 35% of the intensity of ν_{13}, while in PBQ-h_4 this figure is only 10%. The combination mode $\nu_{13} + \nu_5$ is relatively also much more intense in PBQ-d_4 than in PBQ-h_4. The combination mode $\nu_{13} + \nu_6$ however has almost completely disappeared. Some of these intensity redistribution effects may of course be due to the Duschinsky effect [21], e.g., the intensity reversal of ν_{14} and ν_{15} in PBQ-d_4, but the total gain in intensity of the totally symmetric modes cannot be explained by this effect. This can only be due to the fact that the excited state geometry of PBQ-d_4 is different from PBQ-h_4. In fact the increased activity of ν_2 superimposed on ν_{13} suggests the $n\pi^*$ excitation in this molecule to be more localized on oxygen. Such an assumption would also be in agreement with the measured larger ZFS parameter $|D|$ of PBQ-d_4 (see table 7). In section 3.3 we claimed that the isotope effect on the vibronic activity in the phosphorescence spectra might be of some help in determining the "mechanisms" that induce the phosphorescence spectrum of PBQ-h_4. In this section we have shown that large isotope effects on the vibronic activity are observed but the idea is now that these effects are not primarily due to a change in vibrational overlap factors but to a change in electronic wave function of the isotopic species. ENDOR experiments on the lowest triplet state of PBQ-h_4 and PBQ-dh_3 indeed show the triplet-state spin-density distribution to be sensitive to deuteration [22]. At this stage we are therefore unable to draw any firm conclusion regarding the relative importance of Herzberg–Teller versus Born–Oppenheimer vibronic coupling effects that induce the phosphorescence spectrum.

4. Isotope and external heavy atom effect on the ZFS parameters of PBQ

4.1. Absolute level ordering

We first noted the isotope dependence of the ZFS parameters of PBQ-h_4 through the observation of side lines in the optically detected EPR spectrum of PBQ-h_4 in a PBQ-d_4 host crystal. These side lines were interpreted by us as being due to PBQ-dh_3 isotopes and this assignment was confirmed later by an independent synthesis of PBQ-dh_3. It then became important to know if the observed isotope effect (a 20% increase in $|D|$ in the case of PBQ-dh_3) was a peculiarity of the PBQ-d_4 host crystal or that intrinsic molecular effects were responsible for these isotope effects. Moreover the observed isotope effects in the phosphorescence spectra of PBQ-h_4 told us that a knowledge of the concomitant change in the ZFS parameters might be helpful in the interpretation of these spectra. In the course of our ENDOR experiments [22] on PBQ isotopes in isotopic mixed crystals we have measured the ZFS parameters of PBQ-h_4, -dh_3, 2,6-d_2h_2 and -CH_3.

It was also decided that a study of some PBQ isotopes in a *p*-dibromobenzene crystal might be worthwhile, as only in this crystal we would be able to measure both the ZFS parameters of PBQ-h_4 and -d_4. A knowledge of the ZFS parameters of these latter compounds seemed most desirable as they have the same molecular symmetry and therefore electronic interstate mixing effects should be absent. ODMR experiments were performed on single vibronic lines in the emission spectrum and fig. 9 shows the result of such an experiment performed on the b_{1u} C=O stretching mode (at 16953 cm^{-1}) in the phosphorescence spectrum of PBQ-h_4 as a guest (0.3 % conc.) in a PBQ-d_4 host lattice at 1.6 K. An increase in the phosphorescence intensity is observed at 1936 MHz of 41 ± 2% and at 2164 MHz of 12 ± 2%.

However, a third transition at either the sum or difference frequency could not be detected. This ambiguity was resolved by taking an optically detected high field EPR spectrum of this mixed crystal system with the magnetic field direction along the oxygen–oxygen (*z*) direction of one of the PBQ molecules in the unit cell. The result of this experiment is shown in fig. 10 and it is immediately apparent that the third zero-field ODMR transition should have been detected at the difference frequency of the ones observed. Attia et al. [14] reported the first results of

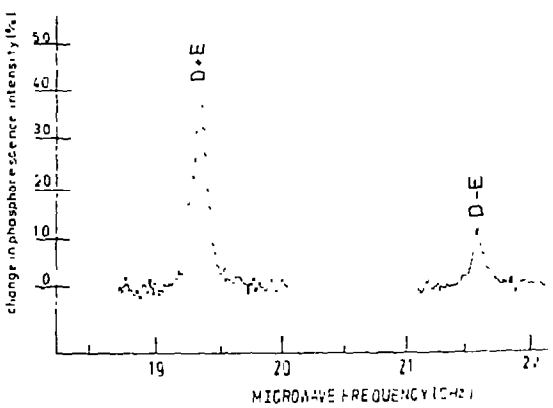

Fig. 9. ODMR spectrum of the lowest triplet state of PBQ-h_4 as guest (0.3 mol %) in a PBQ-d_4 host crystal at 1.6 K. The change in phosphorescence intensity was detected at the b_{1u} C=O stretching mode at 16953 cm^{-1} in the phosphorescence spectrum. The spectrum shown here is the result of averaging about 10000 consecutive sweeps (10 ms per sweep!) through the resonance region.

any ODMR study on PBQ-h_4 in a *p*-dibromobenzene host crystal and in this host crystal the $2E$ transition can be easily observed. From the phosphorescence spectra shown in figs. 6 and 8 it is apparent that the steady state populations of the *y* and *x* spin substates are very much dependent on the host crystal. Temperature dependent high field EPR experiments on the PBQ-h_4 in PBQ-d_4 mixed crystal showed the level ordering of the zero-field spin substates to be such that *z* is highest. The same level ordering has also been reported in the case of benzophenone [23] but in formaldehyde, the precursor of all ketones, *z* is the lowest level [24].

Table 8 contains all the ZFS parameters measured so far in a PBQ-d_4 and DBB host crystal and it is interesting to note that the isotope effect on the ZFS

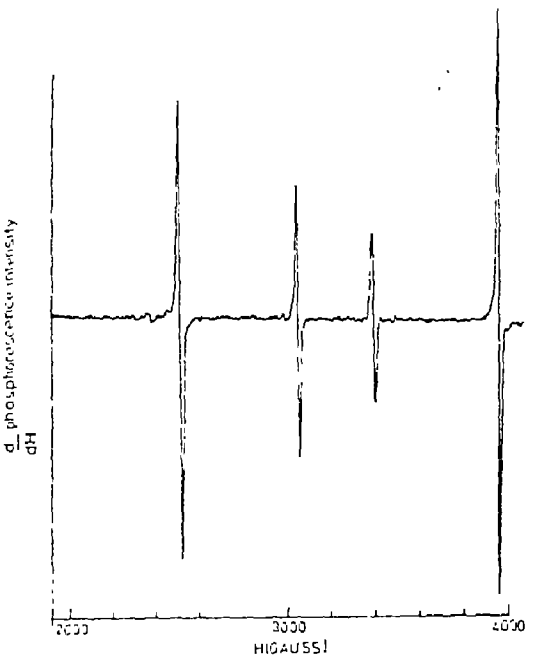

Fig. 10. ODMR spectrum using magnetic field modulation of the lowest triplet state of PBQ-h_4 as guest (1 mol %) in a PBQ-d_4 mixed crystal at 1.8 K. For the outer pair of lines the magnetic field direction is parallel to the long molecular (*z*) axis of one of the PBQ-d_4 molecules in the unit cell and for the inner pair of lines the magnetic field direction is at an angle of 70° to the *z*-axis of the second PBQ-d_4 molecule in the unit cell.

parameters of PBQ-h_4 clearly is a molecular phenomenon. We further hereby confirm the previously reported values of the ZFS parameters of PBQ-h_4 in a DBB host crystal [14].

4.2. Isotope effect on the ZFS parameters of PBQ-h_4

Table 7 shows that there is no systematic increase in ZFS parameter $|D|$ on going from PBQ-h_4 to PBQ-d_4. In fact of the deuterated PBQ species studied so far, PBQ-2,6-d_2h_2 does have the largest $|D|$ parameter. It is clear from the size of the observed effects that the changes in ZFS parameters cannot be explained by a decrease in the out of plane C–H motions upon deuteration as in the case of benzophenone [23] or naphthalene [25]. The remarkable difference between the ZFS parameter $|D|$ of PBQ-h_4 and PBQ-d_4 shows that in the case of the asymmetric PBQ species electronic interstate mixing cannot be the only cause for the observed isotope effects. ENDOR experiments on PBQ-dh_3 in a PBQ-d_4 mixed crystal have shown [22] that in this case the increase in $|D|$ must be interpreted as an increase in localization of the $n\pi^*$ excitation on the carbonyls. This result implies that in all cases the increase in $|D|$ might be the result of localization of the $n\pi^*$ excitation on the carbonyl functions. We believe that this is indeed the case and that this localization is induced by an isotope dependent geometrical change of the lowest excited triplet state in PBQ. This conclusion is in line with the observed increase in activity of totally symmetric modes upon deuteration in the phosphorescence spectrum of PBQ-h_4 (see section 3.4). The question remains why such (minor)geometrical changes introduced by deuteration are able to produce such drastic effects on the ZFS parameters.

Table 7
ZFS parameters in MHz (± 2 MHz) of the lowest $n\pi^*$ triplet state of (isotopically) substituted p-benzoquinone

Species	PBQ-d_4 host crystal a)		DBB host crystal b)	
	D	E	D	E
PBQ-h_4	−2050	+114	−5302	+79
PBQ-dh_3	−2430	+105	−5843	+73
PBQ-2,6-d_2h_2	−3423		−6866	+66
PBQ-d_4			−6474	+63
PBQ-h_3CH_3	−3338	+189	−6457	+90

a) In the case of PBQ-h_3CH_3 we have used PBQ-d_3CH_3 as the isotopic host crystal.
b) The level ordering of the spin substates in the lowest triplet state of PBQ in a DBB host crystal is assumed to be the same as in the PBQ-d_4 host crystal.

The answer to this question must be sought in the contribution of spin–orbit coupling to the ZFS parameters of PBQ. It is well known now [26] that in carbonyl compounds spin–orbit coupling effects among triplet states may give an appreciable or even overwhelming contribution to the ZFS parameters of the lowest excited triplet state. Especially spin–orbit coupling between close lying $n\pi^*$ and $\pi\pi^*$ triplet states leading to one center spin–orbit coupling (SOC) integrals, gives rise to a depression of the x and y spin sublevels of the lower state. Batley and Bramley [27] have calculated the effect of SOC in the one center approximation ignoring groundstate spin–orbit coupling effects and arrive at the following simple expression:

$$\Delta D = -\tfrac{1}{4}\,\xi_0\,\Delta g_{zz}, \qquad (5)$$

in which ΔD symbolizes the contribution of SOC to D, ξ_0 is the spin–orbit coupling constant for oxygen and Δg_{zz} is the deviation of g_{zz} from the free electron value ‡.

For PBQ-h_4, $\Delta g_{zz} = 7.62 \times 10^{-3}$ [22] and with $\xi_0 = 148\ \mathrm{cm}^{-1}$ [28] one calculates $\Delta D = 0.2819\ \mathrm{cm}^{-1}$ (8452 MHz). For PBQ-dh_3 we have measured $\Delta g_{zz} = 8.06 \times 10^{-3}$ [22] which yields $\Delta D = 0.2982\ \mathrm{cm}^{-1}$ (8940 MHz). These results indicate that the increase in $|D|$ on monodeuteration (see table 7) is completely accounted for in this model by a change in the spin–orbit contribution ΔD to the ZFS parameter $|D|$. One should note here that a relatively minor increase (5%) of the π^* electron density on oxygen is able to account for a 20% increase of the ZFS parameter $|D|$ in this case. The simple picture, explaining the isotope effect on the ZFS parameters of PBQ-h_4 that emerges from the above results is the following. The excited state geometry of the lowest triplet state in PBQ is sensitive to isotopic substitution. This in itself results in a (minor)

‡ It is interesting to note that triplet–ground state spin–orbit coupling *does* contribute to the ZFS parameter Z but *not* to g_{zz} as was previously suggested [8].

change of the spin-density distribution in the molecule. The change in spin-density on oxygen induces a change in ZFS parameter $|D|$ through a modulation of the spin–orbit coupling contribution to $|D|$. Further EPR and ENDOR experiments on the asymmetric *p*-benzoquinones are necessary to determine the contribution of electronic interstate mixing to the change in ZFS parameters in these molecules.

4.3. External heavy atom effect on the ZFS parameters of PBQ-h_4

The effect of a heavy atom host on the ZFS parameters of a guest is still a matter of current interest. Cheng and Hirota [29] conclude from a PMDR study of aromatic carbonyls in different types of host crystals, that the main effect of the heavy atom host crystal is to change the electronic gap between the emitting lowest state and a nearby strongly vibronically coupled state. Cheng and Hirota in their PMDR study were concerned with mono-carbonyl aromatics and their strongly coupled states were thought of as being of $n\pi^*$ and $\pi\pi^*$ character. In such a two-state model, a change in ZFS parameter $|D|$ is also expected to be accompanied by a change in the vibrational structure of the phosphorescence spectrum. A comparison of figs. 6 and 8 shows that the main difference in phosphorescence spectrum of PBQ-h_4 in PBQ-d_4 and in DBB is the increased activity of the b_{1u} C=O stretching mode in the latter host crystal. This means that if a change in triplet state mixing is used to explain the observed increase in ZFS parameter $|D|$ of PBQ-h_4 in DBB, the triplet states involved must have similar $n\pi^*$ orbital character. In fact it would mean that the lowest B_{1g} ($n\pi^*$) triplet state of PBQ-h_4 in DBB is heavily mixed with other $n\pi^*$ states that are more localized on the carbonyl functions. The latter suggestion is not weakened by the observation that the decay rate of the *z*-spin sublevel in PBQ-h_4 increases from 10^4 s^{-1} in PBQ-d_4 [8] to 2.9×10^4 s^{-1} in DBB [14].

Especially further ENDOR experiments on PBQ-h_4 in a DBB mixed crystal are necessary to substantiate the localization of the $^3B_{1g}$ ($n\pi^*$) excitation of PBQ-h_4 in this mixed crystal system.

5. Energy migration in *p*-benzoquinone isotopic mixed crystals

5.1. Lifetimes of the individual spin substates

Basic to an understanding of energy migration in *p*-benzoquinone isotopic mixed crystals is a knowledge of the lifetimes of the triplet spin sublevels involved. We have measured the lifetimes of the individual spin sublevels of the B_{1g} ($n\pi^*$) triplet state of PBQ-h_4 as guest (1 mol %) in PBQ-d_4 at 1.8 K, by measuring the decay of individual vibronic bands in the phosphorescence spectrum after dye-laser excitation. The results of these measurements are given in figs. 11 and 13. These figures show that *z* is, by far, the fastest decay channel out of the lowest triplet state in PBQ-h_4.

Previous lifetime measurements on the isotopic mixed crystal system were performed by Koyanagi et al. [13]. These authors reported as the "lifetime" of the lowest triplet state of PBQ-h_4: 6.5×10^{-4} s. As the experiment was performed on the total emission of the *p*-benzoquinone isotopic mixed crystal, this number represents some kind of "average" lifetime of all three spin substates.

5.2. Concentration effects on the phosphorescence spectrum of PBQ-h_4 in PBQ-d_4

In the course of our investigation of PBQ isotopic mixed crystals we observed some interesting concentration and trap depth effects on the phosphorescence spectra of these crystals. Fig. 12 shows some of the phosphorescence spectra that were obtained at 1.8 K by varying the concentration of PBQ-h_4 in PBQ-d_4.

At low guest concentration (0.1 %) emission from the *x*-spin substate is relatively intense but with increasing guest concentration, emission from this level completely collapses. In the 1 mol % PBQ-h_4 in PBQ-d_4 mixed crystal, phosphorescence from both the *y*- and *z*- spin sublevels is relatively intense, while emission from the *x*-spin substate is hardly observable. In the 5 mol % PBQ-h_4 in PBQ-d_4 isotopic mixed crystal, emission from "PBQ-h_4 dimers" occurs (as is obvious from the appearance of an origin) and the dimer vibronic intensity almost solely arises from emission of the *z*-spin substate.

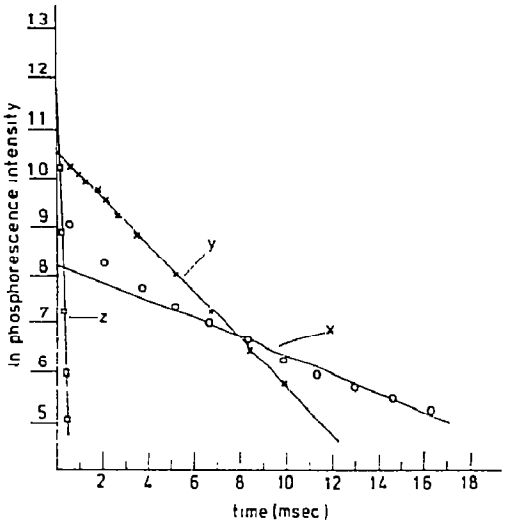

Fig. 11. Decay curves for the individual spin substates of the lowest triplet state of PBQ-h_4 as guest (1 mol %) in a PBQ-d_4 isotopic mixed crystal at 1.8 K. A dye laser was used for excitation and either a Brookdeal boxcar integrator (z) or photon counting techniques (x and y) were used for detection. The experiments were done at the following bands in the phosphorescence spectrum (see fig. 6):

z: ν_{13}, b_{1u} (1656 cm^{-1}),
y: ν_{21}, b_{2u} (414 cm^{-1}),
x: ν_{24}, b_{3u} (904 cm^{-1}).

The initial fast decay underlying the x-spin substate emission is due to (unavoidable) phonon-induced emission arising from the z-spin substate.

In the 60 mol % PBQ-h_4 in PBQ-d_4 mixed crystal the phosphorescence is exclusively caused by "trimers" with again the emission from the z-spin substate being dominant. At even higher proto concentrations (~ 70%) all the sharp phosphorescence almost completely disappears. We have also taken the phosphorescence spectrum of PBQ-h_4 as trap in PBQ-dh_3 at 1.8 K. The emission spectrum under these conditions looks almost identical to the 4.2 K spectrum of PBQ-h_4 in PBQ-d_4 shown in fig. 6.

5.3. *Effect of energy trapping and detrapping on the spin sublevel populations*

A unique feature of the p-benzoquinone phosphorescence spectrum is that all three spin sublevels of the lowest $B_{1g}(n\pi^*)$ triplet state contribute to its formation. The intensity ratio among the modes arising from the different spin sublevels then is an excellent probe to measure the effects of relaxation among and change in population of the individual spin sublevels as, e.g., caused by trapping and detrapping of the excitation. The concentration effects on the phosphorescence spectrum that we observe in the dilute PBQ-h_4 in PBQ-d_4 mixed crystal suggest that even at 1.8 K the PBQ-h_4 trap cannot be considered isolated from the triplet host (PBQ-d_4) exciton band. There are a few obvious conclusions that we can draw from a consideration of the spectra in fig. 12 and the spin-substate lifetimes shown in fig. 12:

(1) In the low guest concentration regime (<1 mol % PBQ-h_4 in PBQ-d_4) at 1.8 K there is no thermal equilibrium among the spin sublevels of the guest excited triplet state.

(2) Thermalization among the spin sublevels of the guest excited triplet state is improved by either increasing the guest concentration in, or decreasing the trap depth of the guest in, or increasing the temperature of the isotopic mixed crystal.

(3) Communication between a guest spin sublevel and the exciton band is more effective the longer the lifetime of the spin sublevel.

These conclusions are confirmed by optically detected EPR experiments showing that with increasing guest concentration the spin polarization effects observed concomitantly decrease.

One additional point regarding the temperature effect on the thermalization should be mentioned here. Lifetime measurements on single b_{1u} vibronic modes in the phosphorescence spectrum of a 1 mol % PBQ-h_4 in PBQ-d_4 isotopic mixed crystal at 4.2 K showed the z-spin substate lifetime at this temperature to be unchanged from its value at 1.8 K (100 μs). This shows that thermalization among the spin sublevels of the guest is not reached by an "intramolecular" g-level spin–lattice relaxation process but through communication with most likely the host (PBQ-d_4) triplet exciton band via the intermediate u-vibronic level.

To be able to further comment upon the energy migration effects in p-benzoquinone isotopic mixed crystals we refer to fig. 13 where the energy level diagram of the PBQ-h_4 trap in the PBQ-d_4 crystal is shown.

The figure shows that although the emitting $B_{1g}(n\pi^*)$ triplet state of the PBQ-h_4 guest is 40 ± 1 cm^{-1} below

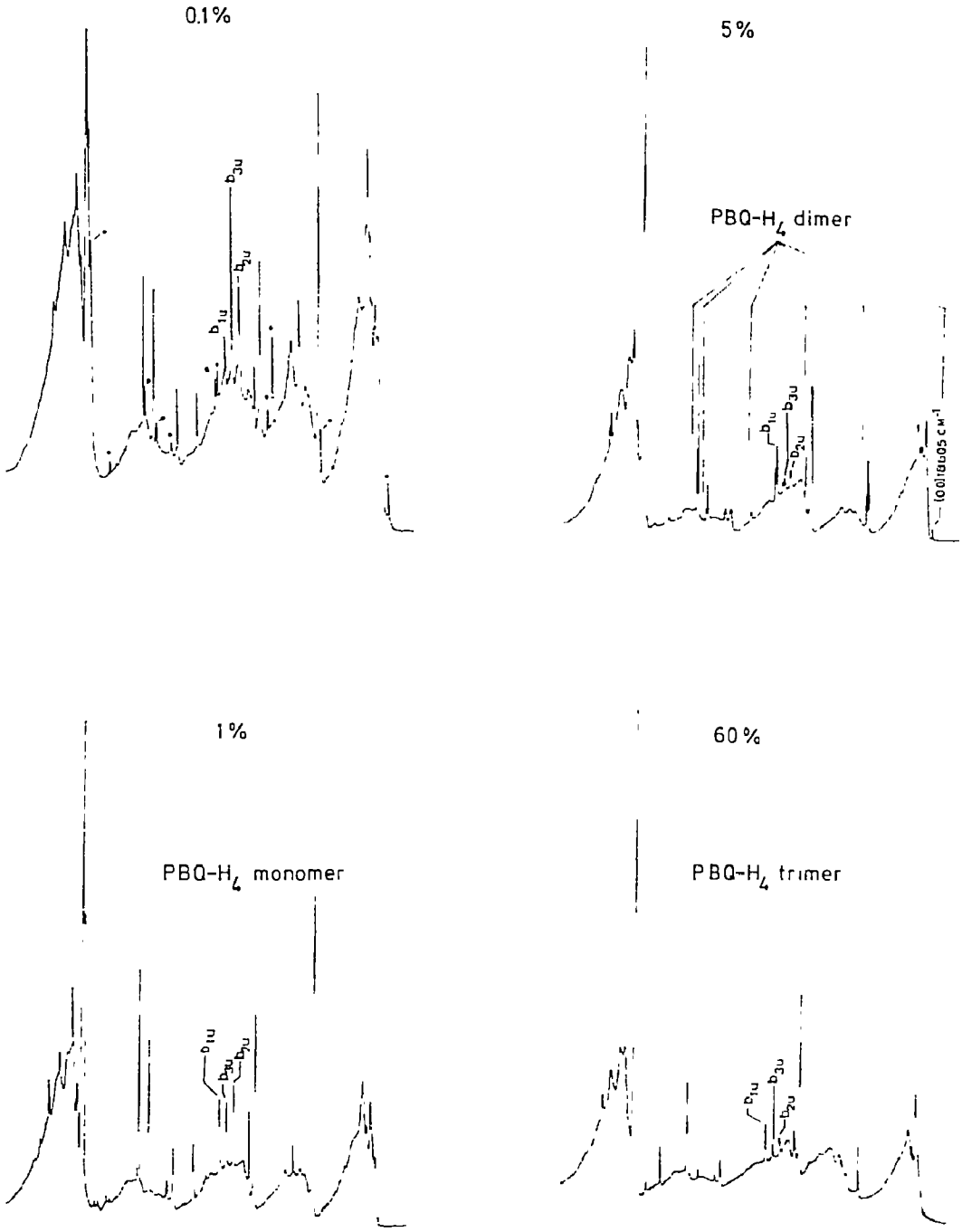

Fig. 12. Phosphorescence spectra of PBQ-h_4 in PBQ-d_4 isotopic mixed crystals at 1.8 K showing the effect of guest (PBQ-h_4) concentration change on the intensity of the b_{1u}, b_{2u} and b_{3u} modes. The relative intensity of these modes reflects the relative steady state populations of the z, y- and x-spin substates of the emitting species. The plus (+) signs in the 0.1 mol % phosphorescence spectrum mark those lines that are due to PBQ-dh_3 impurity emission.

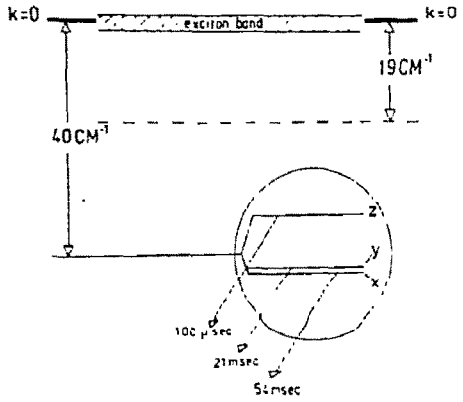

Fig. 13. Energy level diagram showing the positions of the PBQ-h_4 triplet trap levels versus the PBQ-d_4 triplet host exciton band. The level at 40 cm^{-1} below the host (PBQ-d_4) triplet exciton band is the vibrationless electronically excited lowest $B_{1g}(n\pi^*)$ triplet state of PBQ-h_4 and the level 19 cm^{-1} below the exciton band is a PBQ-h_4 molecular level of A_u (vibronic) symmetry. It should be further noted that the ZFS of the PBQ-h_4 triplet state has been expanded (about 120 times) and that the host triplet exciton bandwidth is unknown.

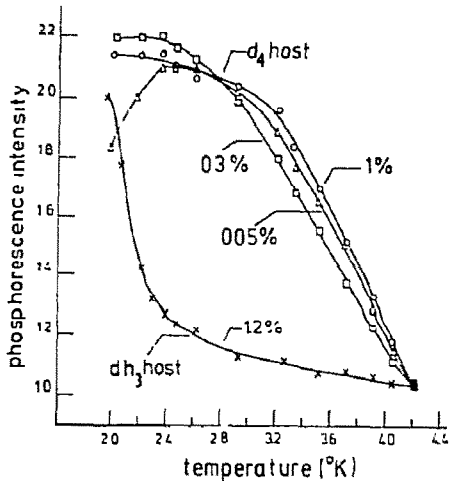

Fig. 14. Phosphorescence intensity versus temperature (PIVT) curves for different guest (PBQ-h_4) concentrations in PBQ-d_4 and PBQ-dh_3 isotopic mixed crystals. It should be further realized that in the PBQ-dh_3 host crystal at 4.2 K no PBQ-h_4 trap emission is observed and therefore that the point presented in the graph at this temperature for this mixed crystal system effectively represents zero. This is of importance when a comparison is made between this PIVT curve and the ones calculated and presented in ref. [30].

the host exciton band, there is an intermediate molecular level of the guest (in the DMP model a vibronic level) only 19 cm^{-1} below the host exciton band. Fayer and Harris [30] have shown that in case of tetra chlorobenzene-d_2 (TCB-d_2) having an exciton bandwidth of 3.5 cm^{-1}, a TCB-hd trap 12.8 cm^{-1} below the exciton band at 2 K was isolated from the band. In the case of the PBQ isotopic mixed crystal, we observe that the x- and y-spin sublevels of a PBQ-h_4 trap at 40 cm^{-1} below the exciton band cannot be considered isolated at 1.8 K. We believe that this effect is not due to a larger exciton bandwidth in the case of PBQ-d_4 but possibly to a higher detrapping rate of the excitation into the band in the case of the PBQ isotopic mixed crystals. This higher detrapping rate in our opinion may be due to the presence of the intermediate level (at 19 cm^{-1} below the band) and the fact that strong electron–phonon coupling effects occur in these PBQ isotopic mixed crystals.

It would be very interesting however to check these suggestions by measuring directly this detrapping rate.

5.4. Exciton band-trap z-level communication effects

So far we have not considered the band-trap communication effects of the z-spin sublevel of the PBQ-h_4 trap in PBQ-d_4. The decay rate of the z-spin sublevel is an order of magnitude faster than the decay rates of the x- and y-spin sublevels and the question of course arises if detrapping and migration are able to effectively compete with this decay in order to establish Boltzmann equilibrium between the z-level and the band. We have tried to answer this question by performing temperature dependent measurements of the *total* PBQ-h_4 trap phosphorescence in PBQ-dh_3 and PBQ-d_4 as host crystals. In the latter host crystal we have also varied the PBQ-h_4 trap concentration.

Fig. 14 shows the result of these measurements and it is seen that the temperature dependence of the PBQ-h_4 trap emission in a PBQ-dh_3 host crystal is completely different from the temperature dependence

of the PBQ-h_4 trap emission in a PBQ-d_4 host crystal. The trap depth of PBQ-h_4 in a PBQ-dh_3 host crystal is at most 10 cm^{-1} and the phosphorescence intensity versus temperature (PIVT) curve in fig. 14 shows a marked change in trap population at 2.2 K. The functional form of this PIVT curve is in fact very similar to those calculated by Fayer and Harris [30] for band-trap systems that are in Boltzmann equilibrium and we tentatively conclude that the z-level of the PBQ-h_4 trap in PBQ-dh_3 in the temperature range between 2.2 and 4.2 K is in or near Boltzmann equilibrium with the host exciton band. Because of the peculiarities of the PBQ-dh_3 host exciton band (section 2.2) we are unable to comment further upon this system. In the PBQ-d_4 crystal the situation is different. At 4.2 K only emission of the z-spin sublevel is observed while at 2 K the emission spectrum also contains modes arising from decaying x- and y-spin substates. The contribution of emission of the latter spin substates to the total phosphorescence however is negligible. The PIVT curves shown in fig. 14 thus only represent the change in z-level population, as the decay rate of this level remains constant in this temperature range. Fig. 14 shows that a change in guest concentration has almost no effect on the PIVT curve. We interpret this as important evidence that in this case the z-level-exciton band system is not in thermal equilibrium over this temperature range, as otherwise profound trap concentration effects on the PIVT curve are expected.

We further interpret the increase in phosphorescence on lowering the temperature as a decrease in detrapping rate of the excitation into the band.

Further "coherent ODMR experiments" [31] on the PBQ-h_4 in PBQ-d_4 mixed crystal system are definitely necessary to improve our understanding of the effects presented here.

6. Experimental

Much effort was devoted to the synthesis and purification of the p-benzoquinones studied. The best results in obtaining isotopic species of PBQ-h_4 were obtained by utilizing an old procedure, described by Willstätter and Dorogi [32] where PBQ is synthesized through oxidation of aniline. Using this procedure we synthesized from the corresponding anilines, PBQ-d_4, -2,6-d_2h_2 and -^{13}C. The synthesis of PBQ-dh_3 was accomplished by starting from bromo-hydroquinone and then following the procedure described by Ziffer et al. [33]. Finally PBQ-h_4 was purchased as such. All quinones were purified by repeated vacuum sublimation over magnesium sulfate and the final purity was checked by NMR and optical methods. Single (isotopic mixed) crystals of PBQ of good optical quality were grown from a Bridgeman furnace by lowering a melt at a rate of 4 mm/h through a temperature gradient of 50 deg. Further cooling of the crystals down to room temperature was done very slowly (4 deg/h) as the PBQ crystals tend to stick to the glass wall of the growing tube. All absorption and emission experiments reported here were performed on a $\frac{3}{4}$ meter 1702 Spex used in the second order with a grating blazed at 1 μ. The slit width utilized in all experiments was such that the width of the absorption and emission bands were not slit width limited. A Molectron DL-200 pulsed dye-laser in combination with a Brookdeal boxcar integrator was utilized to measure the lifetime of the z-spin sublevel of the lowest triplet state of PBQ-h_4 in a PBQ-d_4 host crystal. The decay rates of the x- and y-spin sublevels could only be determined by utilizing dy-laser excitation and photon counting techniques.

7. Summary and discussion

This paper contains the results of optical absorption emission and ODMR experiments on the lowest $B_{1g}(n\pi^*)$ triplet state of p-benzoquinone-h_4 in mixed and isotopic mixed crystals. The effect of isotopic substitution on the properties of the lowest $n\pi^*$ triplet state in PBQ-h_4 are shown to be drastic and this feature is discussed on the basis of a previously proposed double minimum potential model [5] for the lowest excited triplet state. Energy migration effects in the PBQ isotopic mixed crystals have been probed through a study of the guest concentration and temperature effect on the phosphorescence spectra and intensity of these crystals. It is shown that band-trap communication effects are responsible for some of the anomalies observed in the emission spectra.

Before discussing in any more detail the impact of our results on the existing theories that explain the PBQ absorption spectra, we summarize here the more important results obtained from the present study.

(i) asymmetric isotopic substitution induces the electronic origin of the lowest B_{1g} ($n\pi^*$) triplet state in PBQ-h_4 (section 2.1).

(ii) The combined oscillator strength of the "inversion levels" is almost deuteration independent (section 2.1).

(iii) Hydrogen (deuterium) bonding effects cause cluster formations in the heavily doped isotopic mixed crystals (section 2.2).

(iv) The isotope effect on the vibronic structure in the phosphorescence spectra of the *p*-benzoquinines is (partly) due to an isotope dependent excited state geometry (section 3.4).

(v) The isotope effect on the ZFS parameters of the lowest triplet state in PBQ-h_4 is caused by isotope-dependent spin–orbit coupling effects (section 4.2).

(vi) Exciton band-trap communication effects may play an important role in the dynamics of energy migration in the PBQ isotopic mixed crystals (section 5).

So far we have not considered explicitly other interpretations of the absorption spectra of the *p*-benzoquinones besides the one that was based upon the assumed DMP well of the lowest excited triplet state in PBQ-h_4. The reported Stark effects [5,6] on the singlet–triplet absorption spectra of the *p*-benzoquinones unequivocally establish the lowest observed states in the pure crystal, split by 16.9 cm^{-1} in PBQ-h_4, to be of opposite parity. In our opinion this only leaves two possibilities and their difference is directly related to the following question: Is the observed "inversion splitting" an *electronic* or a *vibronic* effect?

In the former case the line at 16.9 cm^{-1} from the unobserved origin of the B_{1g} ($n\pi^*$) triplet state in the pure PBQ-h_4 crystal is assigned as the origin of the ^3A_u ($n\pi^*$) state. This interpretation is in line with the suggested interpretation of the singlet $n\pi^*$ states in PBQ-h_4 made by Dunn and Francis [7] who assumed the B_{1g} and A_u $n\pi^*$ *singlet* states only to be split by a few wavenumbers (3.5 cm^{-1} in PBQ-h_4). This interpretation also seems to be supported by some of our results, especially (i) and (ii). An important and decisive argument in our opinion, against this electronic two-state model is the discrepancy arising between the Franck–Condon envelope of the absorption spectrum of PBQ-h_4 in the gas phase [34] and the solid [1]. In the gas phase the first strong line in the singlet–triplet absorption and emission spectrum of PBQ-h_4 is found at 18682 cm^{-1} [20,34] and this line correlates very well with the observed strong singlet–triplet transition in the PBQ-h_4 crystal at 18943 cm^{-1} [1].

Moreover the origin of the orbitally allowed ^3A_u ($n\pi^*$) state is expected to be relatively intense and a satisfactory analysis of the singlet–triplet absorption spectrum of PBQ-h_4 in this region can be given only when the origin of the ^3A_u ($n\pi^*$) state is placed at 18943 cm^{-1} [11,12]. We must then conclude that the *electronic* inversion splitting in PBQ-h_4 is 340 and not 16.9 cm^{-1}.

This conclusion is also in agreement with recently performed optical absorption experiments on 9,10-anthraquinone where the onset of the second A_u ($n\pi^*$) triplet state is more easily located through the observation of strong interference effects in the region of this state [35]. The splitting between the B_{1g} and A_u $n\pi^*$ triplet states in this molecule was found to be about 350 cm^{-1}. The conclusion of this paper then must be that the inversion splitting observed in PBQ crystals (16.9 cm^{-1} in pure PBQ-h_4) is a vibronic effect and that the previously proposed [5] DMP model for the lowest excited triplet state in PBQ-h_4 (and PBQ-d_4) can be upheld‡. We are however left with a few questions which are:

(1) Why is the exciton inversion splitting (in PBQ-h_4) 4 cm^{-1} smaller than the monomer one (PBQ-h_4 in PBQ-d_4)?

(2) Which (deuteration independent) mechanism induces the u-inversion level?

Further experiments, to determine the exciton bandwidth of the lowest triplet state in PBQ-d_4 crystals, and vibronic intensity calculations are planned to answer these questions.

We have also extended the isotope effect measurements on the ZFS parameters of PBQ-h_4 and showed this to be an intramolecular effect. The effect was interpreted on the basis of a modulation of the spin–orbit contribution to the ZFS parameter D of PBQ through localization of the $n\pi^*$ excitation on oxygen.

‡ We have recently performed Stark–Zeeman experiments on the inversion levels of the lowest triplet state in PBQ-d_4 crystals and found the factor group splitting in the g-inversion level (origin) to be 0.62 ± 0.06 cm^{-1}, while this splitting in the u-inversion level (at 12.1 cm^{-1}) was found to be immeasurable small ($\lesssim$ 0.05 cm^{-1}). This finding again is a strong argument in favour of the DMP model for the lowest triplet state in PBQ. (H. Veenvliet and D.A. Wiersma, submitted for publication in Chem. Phys.)

A relatively minor increase in π^* electrondensity on oxygen (5%) was shown to be able to account for the observed 20% increase in ZFS parameter $|D|$ on monodeuteration.

An interesting question remains why the excited state geometry of PBQ is so sensitive to isotopic substitution. This question will hopefully be answered when the results of detailed ENDOR experiments on PBQ isotopes are available. We have also presented in this paper some preliminary data that concern the energy migration and trapping effects that occur in the isotopic mixed crystals of PBQ. One of the interesting conclusions of the study is that at 4.2 K "thermal equilibrium" among the spin substates is attained through trap–exciton band communication effects.

Acknowledgement

We gratefully acknowledge the help of Philip Vergragt of the University of Leiden in obtaining the zerofield ODMR spectra of the *p*-benzoquinones. The investigations were supported by the Netherlands Foundation for Chemical Research (S.O.N.) with financial aid from the Netherlands Organization for the Advancement of Pure Research (Z.W.O.).

References

[1] J.W. Sidman, J. Am. Chem. Soc. 78 (1956) 2363.
[2] J. Trotter, Acta Cryst. 13 (1960) 86.
[3] H.P. Trommsdorff, J. Chem. Phys. 56 (1972) 5358.
[4] R.L. Fulton and M. Gouterman, J. Chem. Phys. 35 (1961) 1059; 41 (1964) 2280;
M. Gouterman, J. Chem. Phys. 42 (1965) 351.
[5] H. Veenvliet and D.A. Wiersma, Chem. Phys. 2 (1973) 69; Chem. Phys. Letters 22 (1973) 87.
[6] R.M. Hochstrasser, L.W. Johnson and H.P. Trommsdorff, Chem. Phys. Letters 21 (1973) 251.
[7] T.M. Dunn and A.H. Francis, J. Mol. Spectry. 50 (1974) 14.
[8] H. Veenvliet and D.A. Wiersma, J. Chem. Phys. 60 (1974) 704.
[9] H.P. Trommsdorff, Mol. Phys. 24 (1972) 519.
[10] H. Veenvliet and D.A. Wiersma, Proc. 6th Mol. Cryst. Symp. Elmau, Germany (1973) p.89.
[11] K.N. Klump, Ph.D. Thesis, University of Chicago (1968).
[12] A.H. Francis, Ph. D. Thesis, University of Michigan (1969).
[13] M. Koyanagi, Y. Kogo and Y. Kanda, J. Mol. Spectry. 34 (1970) 450.
[14] A.J. Attia, B.H. Loo and A.H. Francis, Chem. Phys. Letters 22 (1973) 537. Although the vibrational analysis of the PBQ-h_4 phosphorescence spectrum in DBB presented in this reference is correct qua assignment, the numerical values of many modes presented in that paper are wrong. This is due to the fact that the u-inversion level was incorrectly taken as the origin of the emission spectrum.

Stark-modulation experiments, recently performed in this laboratory, on the phosphorescence of PBQ-h_4 and PBQ-d_4 in DBB at 1.8 K show the origin (g-inversion level) of emission to be located at 18358.3 cm^{-1} (PBQ-h_4) and 18380.1 cm^{-1} (PBQ-d_4). Temperature-dependent emission studies on these crystals further show the u-inversion level to be located at 18374.2 cm^{-1} (PBQ-h_4) and 18392.8 cm^{-1} (PBQ-d_4).
[15] G. Orlandi and W. Siebrand, J. Chem. Phys. 58 (1973) 4513.
[16] M.S. de Groot, I.A.M. Hesselmann, J. Schmidt and J.H. van der Waals, Mol. Phys. 15 (1968) 17.
[17] T.M. Dunn and A.H. Francis, J. Mol. Spectry. 50 (1974) 1.
[18] S.J. Hunter, H. Parker and A.H. Francis, J. Chem. Phys. 61 (1974) 1390.
[19] E.D. Becker, L. Charney and T. Anno, J. Chem. Phys. 42 (1965) 942.
[20] M.G. Jayswal and R.S. Singh, Spectrochim. Acta 21 (1965) 1597.
[21] L. Duschinsky, Acta Physicochim. U.R.S.S. 7 (1937) 551.
[22] J.H. Lichtenbelt, H. Veenvliet and D.A. Wiersma, to be published.
[23] R.M. Hochstrasser, G.W. Scott and A.H. Zewail, J. Chem. Phys. 58 (1973) 393.
[24] W.T. Rayes, J. Chem. Phys. 41 (1964) 3020.
[25] G.W. Scott, Ph. D. Thesis, University of Chicago, Illinois (1971).
[26] R.M. Hochstrasser and T.S. Lin, J. Chem. Phys. 49 (1968) 4929.
[27] M. Batley and R. Bramley, Chem. Phys. Letters 15 (1972) 337.
[28] R. Hoffman and J.R. Senson, J. Phys. Chem. 74 (1970) 415.
[29] T.H. Cheng and N. Hirota, Mol. Phys. 27 (1974) 281.
[30] M.D. Fayer and C.B. Harris, Phys. Rev. B 9 (1974) 748.
[31] J. Schmidt, Chem. Phys. Letters 14 (1972) 411.
[32] R. Willstatter and S. Dorogi, Ber. 42 (1909) 2147.
[33] H. Zitler, L. Charney and E.D. Becker, J. Chem. Phys. 42 (1965) 915.
[34] J.M. Hollas, Spectrochim. Acta. 20 (1964) 1563.
[35] K.E. Drabe, H. Veenvliet and D.A. Wiersma, unpublished results of this laboratory.